DOI:10.14753/SE.2024.2908

SEMMELWEIS EGYETEM

DOKTORI ISKOLA

# Ph.D. értekezések

# 2908.

# DOHY ZSÓFIA

**A szív és érrendszeri betegségek élettana és klinikuma**
című program

Programvezető: Dr. Merkely Béla, egyetemi tanár

Témavezető: Dr. Vágó Hajnalka, egyetemi docens

DOI:10.14753/SE.2024.2908

# The role of cardiac magnetic resonance imaging in the diagnosis and prognostic assessment of cardiomyopathies causing left ventricular hypertrophy

PhD Thesis

**Zsófia Dohy MD**

Doctoral School of Basic and Translational Medicine

Semmelweis University

Supervisors: Hajnalka Vágó MD, Ph.D

Official reviewers: Attila Pálinkás MD, Ph.D

Katalin Révész MD, Ph.D

Head of the Final Examination Committee:

István Karádi MD, D.Sc

Members of the Final Examination Committee:

Lívia Jánoskúti MD, Ph.D

József Borbola MD, D.Sc

Budapest

2023

DOI:10.14753/SE.2024.2908

**Table of Contents**

DOI:10.14753/SE.2024.2908

DOI:10.14753/SE.2024.2908

DOI:10.14753/SE.2024.2908

**List of Abbreviations**

| | |
|---|---|
| ACC | American College of Cardiology |
| AHA | American Heart Association |
| AL | light chain |
| BSA | body surface area |
| CA | cardiac amyloidosis |
| CMR | cardiac magnetic resonance |
| Conv | conventional evaluation method |
| CS | circumferential strain |
| ECG | electrocardiography |
| ECV | extracellular volume |
| EDV | end-diastolic volume |
| EDWT | end-diastolic wall thickness |
| EF | ejection fraction |
| EMF | endomyocardial fibrosis |
| ESC | European Society of Cardiology |
| ESV | end-systolic volume |
| fQRS | fragmented QRS |
| FD | Fabry disease |
| G | global |
| HCM | hypertrophic cardiomyopathy |
| i | index |
| ICC | intraclass correlation |
| ICD | implantable cardioverter defibrillator |
| LGE | late gadolinium enhancement |
| LS | longitudinal strain |
| LV | left ventricular |
| LVH | left ventricular hypertrophy |
| LVOTO | left ventricular outflow tract obstruction |
| M | mass |
| MD | mechanical dispersion |
| RS | radial strain |

DOI:10.14753/SE.2024.2908

| | |
|---|---|
| RV | right ventricular |
| SCD | sudden cardiac death |
| SD | standard deviation |
| SV | stroke volume |
| TB | threshold-based evaluation method |
| TPM | trabeculae and papillary muscles |
| VT | ventricular tachycardia |

# 1. Introduction

## 1.1. Hypertrophic cardiomyopathy

According to the World Health Organization’s definition and classification, published in 1980, cardiomyopathies are primary structural and functional heart muscle disorders of unknown cause that are not explained by coronary artery disease or flow abnormalities, or are not caused by underlying systemic disease (1). Since then, this definition has been amended several times. The American Heart Association's (AHA) 2006 classification of cardiomyopathies distinguishes between two major groups, primary and secondary cardiomyopathies based on etiology, and then further subdivides these into subgroups based on phenotype (2). The World Heart Federation published in 2013 the MOGE(S) classification that addresses five attributes of a cardiomyopathy, including morphofunctional characteristic (M), organ involvement (O), genetic or familial inheritance pattern (G), etiology (E), and optionally information about the functional status (S) (3). In the 2008 classification of the European Society of Cardiology (ESC) and adopted in the 2014 guidelines on the diagnosis and management of hypertrophic cardiomyopathy (HCM), cardiomyopathies were grouped into morphofunctional phenotypes included dilated, hypertrophic, restrictive, and arrhythmogenic right ventricular cardiomyopathy and unclassified variety, regardless of their etiology (except myocardial dysfunction secondary to hypertension, coronary artery disease, valve disease and congenital heart disease). Thus, in addition to genetic diseases primarily affecting only the heart muscle, based on the ESC classification, the HCM group includes various systemic disorders such as storage diseases (e.g. Pompe disease, Danon disease, Anderson-Fabry disease), mitochondrial diseases, syndromes associated with myocardial hypertrophy (e.g. Noonan syndrome, Friedreich's ataxia) and various types of amyloidosis (4,5). However, as both the treatment and prognosis of these diseases differ, their differential diagnosis remains of great importance.

Cardiomyopathies causing hypertrophy are most often caused by mutations in the gene encoding a sarcomere protein (40-60%) or of unknown origin (25-30%) (6,7). In the traditional sense, these cases are referred to as HCM. The 2020 AHA/ACC (ACC: American College of Cardiology) Guideline for the diagnosis and treatment of patients with HCM states that other cardiac or systemic diseases capable of producing left

ventricular hypetrophy (LVH) should not be labeled as HCM. They use a definition of HCM as a disease state characterized predominantly by LVH in the absence of another cardiac, systemic, or metabolic disease capable of producing the magnitude of hypertrophy evident in a given patient and for which a disease-causing sarcomere (or sarcomere-related) variant is identified, or genetic etiology remains unresolved (8). In my Thesis, I follow this definition of HCM.

### 1.2. Diagnosis

#### 1.2.1. Signs and symptoms

Many patients with HCM have minor or no symptoms, and the disease is diagnosed incidentally or as a result of screening. Symptoms such as chest pain, dyspnoea, palpitation, presyncope or syncope are more common in patients with left ventricular outflow tract obstruction (LVOTO) and are often associated with physical activity, but may also be due to arrhythmias and heart failure. Clinical history includes detailed family history to identify relatives with diagnosed HCM, sudden cardiac death (SCD), heart failure of unknown origin, heart transplantation, implantable cardioverter defibrillator (ICD) implantation. With physical examination, HCM patients may have systolic murmur (at rest or during provocative maneuvers), abnormal carotid pulse, and a fourth heart sound. Those without LVOTO may have a normal physical examination (9).

#### 1.2.2. Electrocardiography

Structural myocardial changes in HCM may also be associated with electrical abnormalities. Non-specific abnormalities may be detected on a standard 12-lead electrocardiography (ECG), such as signs of hypertrophy, pathological Q waves, and ST- and T wave abnormalities (10).

The most commonly used ECG criteria for LVH are based on the measurement of QRS amplitudes. The widely used Sokolow-Lyon criterion is based on the sum of S V1 and R V5 or R V6 (positive score ≥3.5 mV) (11). The sum of S V3 and R aVL is referred to as the Cornell voltage criterion, which indicates LVH ≥2.8 mV for men and ≥2.0 mV for women (12). The point score of Romhilt and Estes incorporates ECG abnormalities, as

shown in Table 1, 4 point indicates probable LVH and ≥5 points indicates definitive LVH (13).

***Table 1****: The point score of Romhilt and Estes*

| ECG Criteria | Points |
|---|---|
| Voltage criteria (any of)<br>1. R or S in limb leads ≥ 20 mm<br>2. S in V1 or V2 ≥ 30 mm<br>3. R in V5 or V6 ≥ 30 mm | 3 |
| ST-T abnormalities<br>• Without digitalis<br>• With digitalis | <br>3<br>1 |
| Terminal negativity of P in V1 ≥ 0.01 mV and ≥ 0.04 s | 3 |
| Left axis deviation ≥ -30° | 2 |
| QRS duration ≥ 0.09 s | 1 |
| Intrinsicoid deflection in V5 or V6 > 0.05 s | 1 |

The diagnostic accuracy of the different ECG hypertrophy criteria seems to be variable in patients with HCM according to different studies. While the sensitivity of the various criteria is generally quite low, the specificity is quite high (14–16).

Patchy mid-myocardial fibrosis is typical in HCM in the hypertrophic segments (17). Pathological Q waves are considered to be a sign of myocardial scarring, but in HCM pathological Q waves seem to be associated with asymmetric hypertrophy rather than myocardial fibrosis (18). Initial data suggest that fragmented QRS (fQRS) complexes are more sensitive than pathological Q waves for detecting regional myocardial scarring (19–21).

LVH and myocardial fibrosis can alterate repolarization resulting in ST segment and/or T-wave abnormalities on ECG. Apical involvement of HCM can associate with giant negative T wave inversion in the precordial and/or inferolateral leads (22). Strain pattern, defined as a descending ST-segment depression of ≥1 mm with an inverted asymmetrical T wave opposite to the QRS axis in at least two contiguous leads, is also a known ECG sign of HCM (23,24).

### 1.2.3. Echocardiography

Echocardiography is the primary imaging modality in HCM patients. Determining the degree of LVH is key to the diagnosis. The diagnostic criterion of HCM is a maximal end-diastolic wall thickness (EDWT) of ≥15 mm anywhere in the left ventricle, or a ratio of maximal apical to posterior wall thickness ≥ 1.5 in case of hypertrophy predominating in the LV apex, in the absence of another cause of hypertrophy in adults. In the case of a family history of HCM, or in conjunction with a positive genetic test, more limited hypertrophy (13–14 mm) can be diagnostic (5,8,25). In addition to determining hypertrophy pattern, echocardiography plays an important role in assessing left ventricular (LV) systolic and diastolic function, LV apical aneurysms, presence and severity of LVOTO, and mitral valve function. The presence of a peak LVOT pressure gradient of ≥30 mmHg at rest or during physiological provocation is considered to be indicative of obstruction. A gradient of ≥50 mmHg is usually considered to be haemodynamically significant (5,8).

### 1.2.4. Cardiac magnetic resonance

Cardiac magnetic resonance (CMR) is the reference method to evaluate left (LV) and right (RV) ventricular volumes and masses (26). In addition to detailed morphological and functional analysis, CMR also provides tissue specific information about the myocardium, making it a key tool in the diagnosis of myocardial diseases. CMR is a dynamically evolving imaging modality, and with newer methods, it allows increasingly accurate diagnosis.

LVH is usually characterized by EDWT, however, LV mass (LVM) may more accurately describe hypertrophy. CMR-based conventional (Conv) quantification of LVM is carried out with epi- and endocardial contouring along the outer and inner border of the compact myocardium, resulting in the trabeculae and papillary muscles (TPM) being included in the ventricular cavity. Due to the high spatial resolution and excellent myocardial-blood contrast, CMR allows evaluation of small myocardial structures like TPM (27,28). Threshold-based (TB) methods define the endocardial surface based on the different signal intensities of blood and myocardium; thus, the TPM are measured as part of the

ventricular mass (***Figure 1***) (29). There is no consensus on which evaluation method is more reliable in the case of HCM (30).

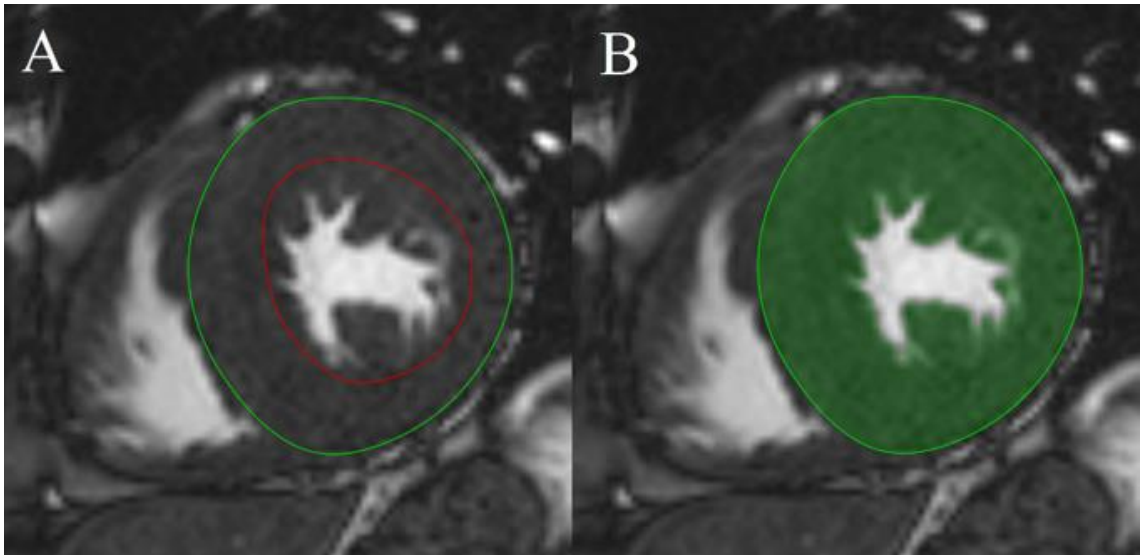


***Figure 1****: CMR images of a patient with septal HCM. Measurement of LVM with conventional (A) and threshold-based (B) methods. (source of the figure: Semmelweis University, Heart and Vascular Center. Modified from of a previously published figure (82))*

A newer measurement method to characterize myocardial deformation in different directions during the cardiac cycle is strain analysis, which reliably describes global and regional myocardial function, and is an early marker of myocardial dysfunction. The damage in different myocardium layers affects certain directions of deformation that can be detected using this method even with normal ejection fraction (EF). Because of myocardial disarray and fibrosis, myocardial contraction in HCM is heterogeneous. Mechanical dispersion (MD) assessed by strain measurement reflects on this heterogeneous contraction (31). Feature-tracking CMR has been validated for strain measurement using standard cine CMR images (32–34).

The typical pathological features of HCM include myocyte disarray, small-vessel disease, and myocardial fibrosis, which usually have a patchy mid-myocardial distribution in the hypertrophic segments (17). With contrast-enhanced CMR, the pattern of fibrosis can be analysed on late gadolinium enhancement (LGE) images and it also allows quantification of the amount of fibrosis (***Figure 2***) (35). The novel parametric mapping techniques measure the T1, T2 or T2* relaxation time of the myocardium which allows a quantitative

characterisation of myocardial changes even without contrast injection. While LGE images are primarily used to detect focal lesions, mapping techniques are able to characterise diffuse myocardial changes. These changes include intracellular disturbances in cardiomyocytes (e.g. glyco-sphingolipid accumulation in Anderson-Fabry disease), extracellular disturbances in the myocardial interstitium (e.g. myocardial fibrosis) or both (e.g. myocardial edema). Using a contrast agent, native and post-contrast T1 mapping allow measurement of myocardial extracellular volume (ECV) (36).

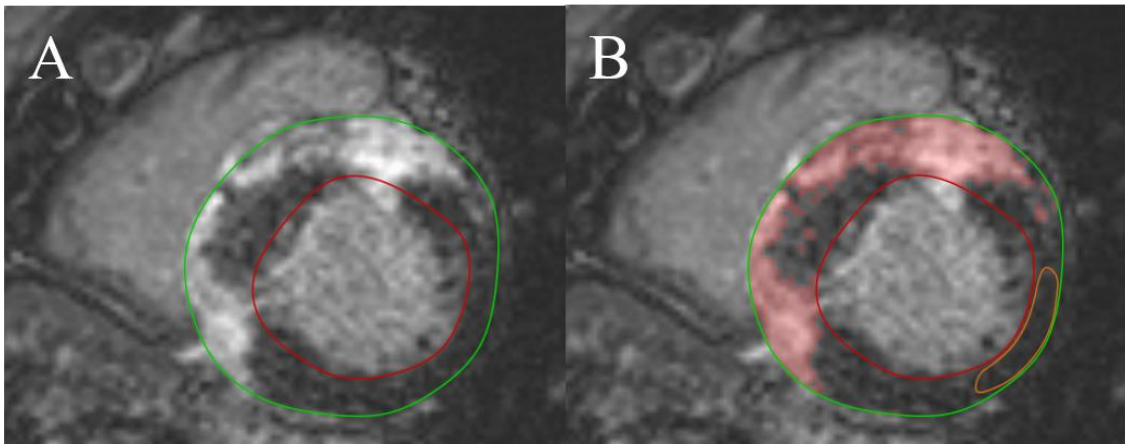


***Figure 2****: Delayed contrast enhancement images in the short-axis plane of a patient with septal HCM. Quantification of myocardial fibrosis (B). (source of the figure: Semmelweis University, Heart and Vascular Center. Modified from of a previously published figure (81))*

### 1.2.5. Genetics and family screening

HCM is inherited as an autosomal dominant trait in most cases, with a 50% chance of transmission (37). To discover familial inharitance, taking a 3-generation family history is recommanded. Genetic testing can confirm the diagnosis, using gene panels with the 8 known HCM-related sarcomere genes, including MYH7, MYBPC3, TNNI3, TNNT2, TPM1, MYL2, MYL3, and ACTC1, a disease-causing variant can tipically be identified in approximately 30% of sporadic and 60% of familial cases (38). If a pathogenic or likely pathogenic gene variant is identified in the proband, cascade genetic testing of at-risk family members is recommended to identifiy those who carry the disease-causing variant and require ongoing surveillance (5,8). Genetic testing can also help the differentiation HCM from HCM phenocopies including glycogen storage disease, Fabry disease, Danon disease, transthyretin amyloidosis.

### 1.3. Differential diagnostic aspects

In the background of increased LV wall thickness or hypertrophy, several primary and secondary causes can be detected in addition to HCM, such as infiltrative myocardial diseases, syndromes associated with LVH, pressure overload of LV, or physiological sport adaptation (5). Untreated hypertension or significant aortic valve stenosis often underlie LVH most commonly with concentric distribution (39,40). Distinguishing these conditions from cardiomyopathies causing LVH is often a challenge. An echocardiographic examination to assess the severity of aortic valve stenosis and knowledge of the patient's medical history is essential, the role of CMR examination is secondary to their diagnosis. In highly trained athletes, physiological LVH is often observed due to sport adaptation, which is characterised by concentric distribution, lack of pathological myocardial fibrosis, reversibility, and correlation with elevated ventricular volumes (41). In my Thesis, I focus on the diseases causing LVH, in the diagnosis of which CMR plays a major role. In the following section, I endevour to give a brief description of the myocardial diseases that cause LVH, which are also included in my research on the role of CMR in differential diagnosis.

#### 1.3.1. Cardiac amyloidosis

In amyloidosis, abnormal proteins are deposited in the extracellular space, which can be a localised disease affecting one organ or a systemic form affecting a large part of the body. The three most common forms of amyloidosis – AL-, TTR- and AA-amyloidosis – can all affect the heart. In AL-amyloidosis, monoclonal light chains are the basis of the deposited amyloid, and the underlying cause is bone marrow plasma cell disease. In TTR-amyloidosis, transthyretin is produced in the liver (mutation type or wild type). AA-amyloidosis is associated with chronic disease, with serum amyloid protein A being the main component of amyloid. Renal involvement and gastrointestinal involvement are common in AL- and AA-amyloidosis, TTR-amyloidosis is often associated with polyneuropathy and carpal tunnel syndrome (42).

According to the Expert Consensus Recommendations published in 2020, cardiac amyloidosis (CA) can be diagnosed if endomyocardial biopsy is positive for CA, or extracardiac biopsy proves amyloidosis and typical cardiac imaging features are present

as discussed below (43,44). Characteristics of CA include thickening of the LV and RV walls (>12 mm for LV EDWT), enlarged atria, thickened papillary muscle and valves, apical sparing assessed with strain analysis, pericardial and pleural effusion, and reduced diastolic and/or systolic function. In the majority of cases, CA causes concentric LVH, but eccentric or asymmetrical hypertrophy and normal geometry have also been described (45). Increased EDWT in present of a normal or low QRS voltage on ECG is suggestive of CA (46). With strain analysis, a typical sign of CA is apical sparing, in which basal longitudinal strain (LS) is severely impaired while apical LS is relatively spared (43,44). A granular sparkling appearance of the myocardium with echocardiography is described as a sign of CA, but it is not considered a highly specific finding. The deposition of amyloid in the myocardium increases the amount of extracellular space, leading to contrast enhancement on LGE CMR. The characteristic LGE pattern in CA is a circular subendocardial or transmural enhancement, which mostly affects the basal segments. In a proportion of cases, contrast enhancement may be detected in both ventricles and atria (***Figure 3***) (47–49). Abnormal contrast kinetics, myocardial nulling prior to blood pool nulling are also typical for CA. Myocardial amyloid deposition causes increased T1 mapping and ECV values assessed by CMR mapping measurement (50–52). Bone scintigraphy can also help the diagnosis of CA even without histological diagnosis; 99mTc-labeled diphosphonate and pyrophosphate compounds diagnose TTR-CA with high sensitivity and specificity (53).

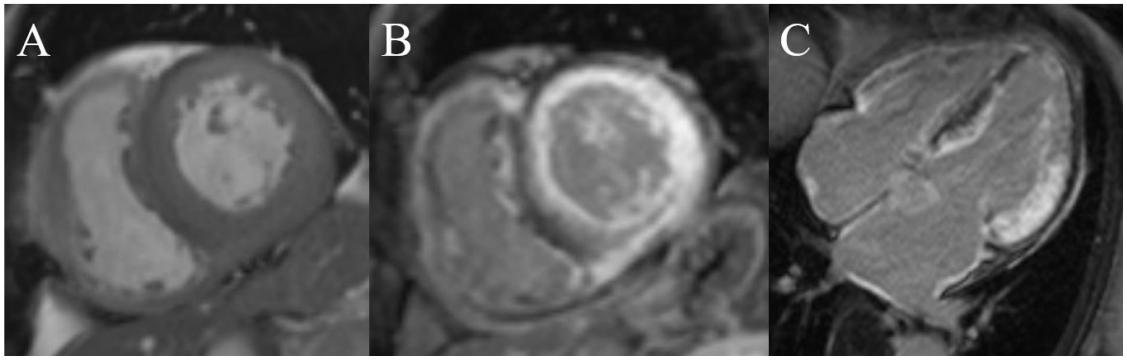


***Figure 3:*** *CMR images of a patient with CA. A) Short-axis slice in end-diastolic phase representative for concentric LVH and hypertrophic RV wall. B-C) LGE images in short-axis (B) and 4-chamber (C) views with circular subendocardial LGE in the LV, in the RV and in the atria. (source of the figure: Semmelweis University, Heart and Vascular Center, Modified from of a previously published figure (80))*

### 1.3.2. Fabry disease

Fabry disease (FD) is an X-linked lysosomal storage disease with various organ manifestations, including nervous system (neuropathic paint, ischemic stroke), dermatological (angiokeratomas), gastrointestinal, renal, ophtalmological (cornea verticillata, retinal vasculopathy, cataract) involvement (54). Cardiac manifestations include the development of LVH with or without heart failure symptoms, conduction abnormalities typically with the shortening of PQ interval, arrhythmias and uncommonly SCD (55,56). Cardiac imaging can be used to monitor for the development of cardiac manifestation of a confirmed diagnosis, or may suggest a diagnosis of FD which can be proved with enzyme and/or genetic testing. FD patients typically have concentric LVH, however, asymmetrical septal hypertrophy, or even apical hypertrophy have already been described (57,58). While echocardiography is often nonspecific because of overlap in LVH phenotypes, CMR with LGE and mapping measurement may suggest a specific diagnosis. The typical pattern of LGE is a midmyocardial enhancement in the basal inferolateral segment (***Figure 4***). The glycosphingolipid accumulation in the cardiomyocytes results in a low T1 mapping time, which helps to distinguish FD from other diseases with LVH. However, if myocardial fibrosis is present, it may result in a pseudonormalization of native T1 times (59).

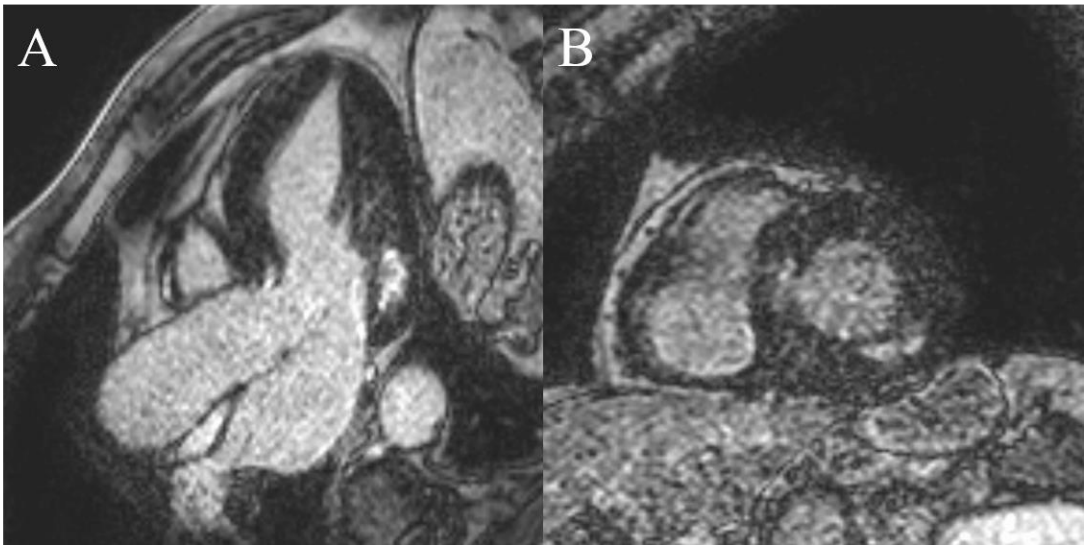


***Figure 4:*** *LGE CMR images of a patient with FD in a 3-chamber (A) and a short-axis (B) view. Midmyocardial contrast enhancement in the basal inferolateral segment. (source of the figure: Semmelweis University, Heart and Vascular Center. Modified from of a previously published figure (80))*

DOI:10.14753/SE.2024.2908

### 1.3.3. Endomyocardial fibrosis

Hypereosinophilic syndrome is group of hematologic disorders leading to eosinophil-driven tissue damage in different organs. Organ involvement depends on the underlying ethiology. Multiple organs may be involved, as lung (e.g. eosinophilic asthma, bronchitis, pneumonia), eye (conjunctivitis), connective tissue, gastrointestinal tract (e.g. eosinophilic esophagitis, gastritis, enteritis, colitis, hepatitis, pancreatitis), skin (dermatitis) (60). It affects the heart in 40-50% of cases, most commonly causing endomyocardial fibrosis (EMF), also known as Löffler's endocarditis. There are usually three stages of the disease: the first, usually asymptomatic stage is acute necrosis and eosinophilic infiltration. This is followed by thrombotic accumulation, which can affect both ventricles but most commonly occurs in the apex of the LV. Finally, the fibrotic stage develops, leading to restrictive cardiomyopathy. The fibrotic, thrombotic accumulation in the LV cavity causes wall thickening and results in a characteristic LGE pattern with CMR observed in the endocardium mainly in the apex and eventually in the subvalvular region of the LV (***Figure 5***) (61,62).

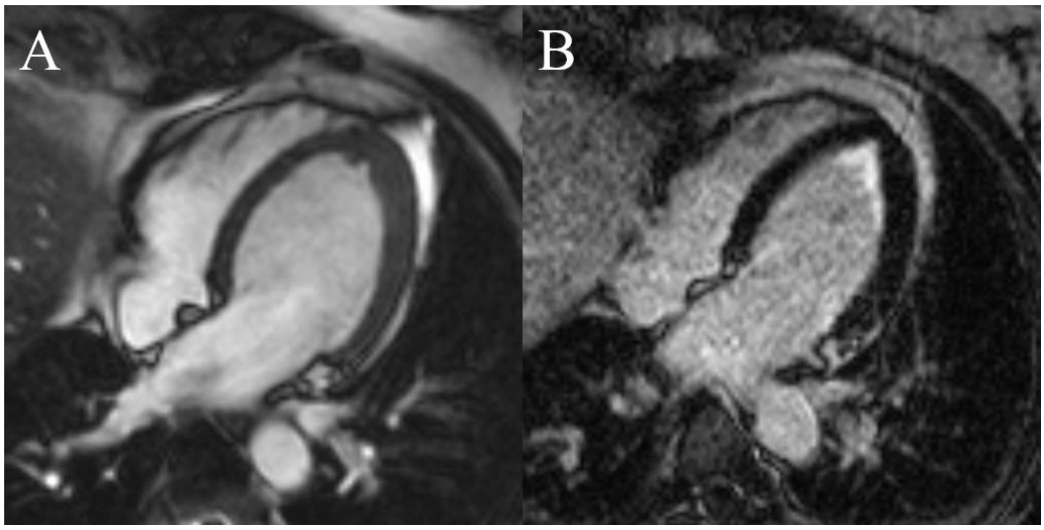


***Figure 5:*** *CMR images of a patient with EMF. A) 4-chamber view in end-diastolic phase, thickening of LV apical wall. B) LGE image in 4-chamber view, endocardial fibrosis in the LV apex. (source of the figure: Semmelweis University, Heart and Vascular Center. Modified from of a previously published figure (80))*

### 1.4. Risk assessment

Although for many patients HCM does not limit life expectancy and the disease is present asymptomatically without the need for major therapy, others may experience severe complications. Patients with pathogenic sarcomeric gene variants or those diagnosed early in life have higher risk of adverse events (38). HCM-related adverse events include SCD, symptoms because of LVOTO, heart failure symptoms associated with diastolic or systolic dysfunction, and atrial fibrillation with risk of thromboembolic stroke. Thanks to SCD risk stratification strategies and contemporary cardiovascular therapies and interventions, the mortality rate of HCM has been reduced to less than 1%/year (63,64).

According to the latest 2020 AHA/ACC guideline on HCM, SCD risk assessment at the initial visit and repeated every 1 to 2 years is recommended. The SCD risk stratification is based on age (stable, older patients have lower risk); personal history of cardiac arrest or sustained ventricular tachycardia (VT); family history of SCD or sustained VT definitively or likely attributable to HCM; continuous ambulatory ECG monitoring for sustained or non-sustained VT; history of syncope likely caused by arrhythmia; and cardiac imaging findings as EDWT, EF, and presence of apical aneurysm. The Guideline recommend contrast-enhanced CMR if a patient does not have evidence of increased SCD risk after assessment with family and personal history, echocardiography, and ambulatory monitoring, or risk stratification otherwise remains uncertain. CMR imaging can provide further characterisation of EDWT, EF, apical aneurysm, and presence and extent of LGE. ICD implantation is recommended for HCM patients with previous SCD or sustained VT. It is reasonable to offer an ICD for HCM patients with at least one major risk factors as follows: 1) SCD related to HCM in a close relative at ≤50 years of age; 2) EDWT ≥30 mm in any LV segment; 3) Recent episodes of syncope suspected to be arrhythmic; 4) LV apical aneurysm; 5) LVEF <50%. ICD may be considered in patients with extensive LGE by contrast-enhanced CMR or non-sustained VT present on ambulatory monitoring. For extensive LGE a cut-off of ≥15% of the LVM is recommended as representing a significant increase in SCD risk, however, there is no consensous on the optimal quantification method of LGE, which may lead to different results (8).

The 2014 ESC guideline on HCM provides a SCD 5-year risk calculator that takes into account age, family history of SCD, EDWT, LVOT gradient, left atrial diameter,

unexplained syncope, and non-sustained VT. This formula does not contain newer markers of SCD risk, including systolic dysfunction (EF <50%), apical aneurysm, and LGE. According to the ESC guideline, ICD implantation is recommended in patients after aborted SCD or sustained VT; and ICD implantation should be considered in patients with an estimated 5-year risk of SCD of ≥6% (5).

In the recent 2022 ESC guideline on the prevention of SCD, the risk stratification of HCM has been completed with newer factors. In addition to using the SCD 5-year risk calculator, the new guideline recommends to consider ICD implantation in patients with significant LGE at CMR (≥15% of LVM); or LVEF <50%; or abnormal blood pressure response during exercise test (a failure to increase systolic pressure by at least 20 mm Hg from rest to peak exercise or a fall of >20 mm Hg from peak pressure); or LV apical aneurysm (***Figure 6***); or presence of sarcomeric pathogenic mutation (65).

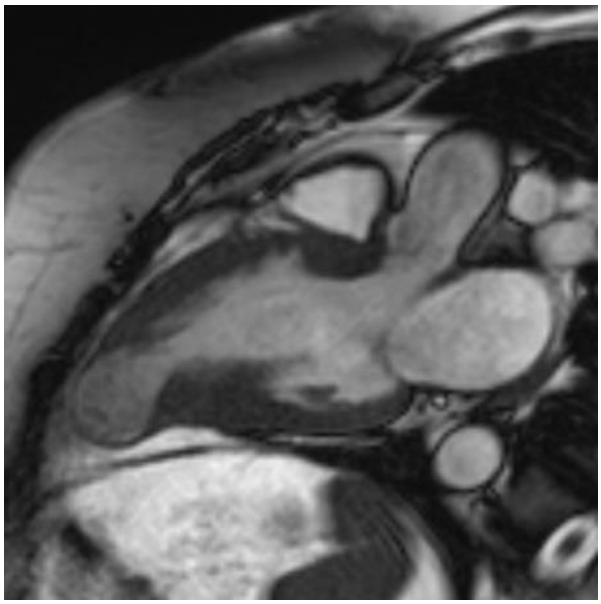

***Figure 6:*** *Midventricular HCM with apical aneurysm. (source of the figure: Semmelweis University, Heart and Vascular Center. Modified from of a previously published figure (80))*

## 2. Objectives

The main objectives of our sudies were to investigate the morphological and functional characteristics, and the prognosis of cardiomyopthies causing LVH using standard and novel CMR techniques.

### 2.1. Investigating CMR quantification methods for assessing left and right ventricular parameters

While CMR is the reference method to evaluate LV and RV functions, volumes and masses, there is no widely accepted method for the quantitative analysis of TPM. CMR-based quantification of LVM can be carried out with different evaluation methods; during the conventional evaluation method TPM is included in the ventricular cavity, while threshold-based method measures TPM as part of the LVM.

The aim of our first study was to investigate the effect of TPM quantification on LV and RV parameters in a normal cohort and the reproducibility of the conventional and threshold-based methods between three independent observers with varying experience in utilizing CMR.

### 2.2. Defining the role of CMR in the differential diagnosis of myocardial diseases causing LVH

CMR diagnosis of myocardial diseases is traditionally based on the morphological features and the pattern of LGE (66–68). Despite the advantages of CMR imaging in the diagnosis of myocardial diseases with LVH, there is a lack of comprehensive studies with large study populations that have investigated the role of CMR-based strain analysis in this patient population.

Therefore, we conducted a study with the aim of investigating the differential diagnostic and prognostic importance of feature-tracking strain analysis in patients with LVH caused by myocardial disease.

### 2.3. Defining the electrocardiographic predictors of LVH and myocardial fibrosis in HCM

The structural changes characteristic of HCM, such as LVH and myocardial fibrosis, are associated with different ECG abnormalities (5,10). The ECG voltage can be affected in a contradictory way by the degree of myocardial hypertrophy and the extent of fibrosis. In addition to pathological Q waves, fQRS is also considered an ECG sign of myocardial scarring (19,20), however, limited data are available regarding the diagnostic value of fQRS for the detection of myocardial fibrosis in HCM (21,69). Due to myocardial fibrosis, not only depolarization but also repolarization can be affected (21,24,70,71).

The aim of our third study was to investigate the diagnostic accuracy of ECG hypertrophy criteria, the impact of myocardial fibrosis on these criteria, and to define ECG predictors of LVH and myocardial fibrosis in patients with HCM.

### 2.4. Defining the prognostic significance of CMR-based markers in patients with HCM

According to the guidelines in force at the time of the research, CMR examination is not a necessary primary tool for SCD risk stratification in HCM (5,72), however, data in the literature suggest an additional prognostic role of the detection and quantification of myocardial fibrosis (73,74). Limited data are available on whether CMR-based strain analysis has incremental prognostic value in patients with HCM (75,76). Therefore, we conducted a study with the aim of investigating the prognostic signifcance of LVH assessed with conventional and threshold-based evaluation methods, functional parameters, and the amount of myocardial fibrosis.

# 3. Methods

## 3.1. Study design, study populations

### 3.1.1. Left and right ventricular parameters quantified with conventional and threshold-based methods

A total of 30 male and 30 female Caucasian healthy individuals (age 25.6±4.7 years) underwent CMR imaging, who were free of complaints and had no known cardiovascular diseases based on a uniform patient questionnaire focusing on cardiovascular diseases and risk factors, and on a detailed medical check-up included physical examination, 12-lead resting ECG and echocardiography examination.

Three independent observers evaluated CMR images both with conventional and threshold-based methods. The most experienced reader had 15 years of experience with more than 5000 original CMR cases and Level 3 certification proved by the European Association of Cardiovascular Imaging. The mid-experienced reader had more than 800 individual original CMR cases during the last 5 years and low-experienced reader independently analyzed ca. 120 CMR cases.

### 3.1.2. Differential diagnosis of myocardial diseases causing left ventricular hypertrophy

We retrospectively identified all patients with myocardial disease causing LVH or increased LV wall thickness who were referred to The Heart and Vascular Center of Semmelweis University between 2009 and 2019 for CMR examination (n=430). Patients with untreated hypertension, significant aortic stenosis, or athletes with LVH due to physiological sport adaptation were not involved in the study. Patients with previous kidney transplantation (n=2), unsuitable strain analysis (n=9) or an uncertain CMR-based diagnosis (n=15) were excluded from the study. All together, 330 HCM patients, 46 CA patients, 12 FD patients and 16 EMF patients were involved in the study.

The all-cause mortality of the patients was analyzed based on the National Health Insurance Fund of Hungary record database, which includes up-to-date information on death.

The CMR diagnosis was made based on the extracted morphologic features and LGE pattern and was compared to the patient's history. The diagnosis of HCM was based on the finding of a maximal wall thickness ≥ 15 mm in any myocardial segment or a ratio of maximal apical to posterior wall thickness ≥ 1.5 in case of hypertrophy predominating in the LV apex, if no other reason was found causing LVH. In the case of a family history of HCM, in first-degree relatives, the diagnosis of HCM was based on the presence of otherwise unexplained increased wall thickness ≥13 mm. The diagnosis of CA was confirmed by biopsy and CMR features consistent with cardiac involvement as following: LV wall thickness >12 mm; diffuse LGE; abnormal gadolinium kinetics typical for CA. The diagnosis of FD was proved with enzyme and/or genetic testing. The CMR features of cardiac involvement of FD included LVH with or without a typical pattern of LGE in the basal inferolateral segment with midmyocardial distribution. In case of EMF, LGE was observed in the endocardium mainly in the apex and eventually in the subvalvular region of the LV. For all patients, the CMR diagnosis was approved by one of two consultants with >10 years of experience in performing CMR with a European Association of Cardiovascular Imaging CMR level 3 certification.

### 3.1.3. Electrocardiographic predictors of LVH and myocardial fibrosis in HCM

We enrolled 146 HCM patients who underwent CMR examinations and a standard 12-lead ECG at the Heart and Vascular Center of Semmelweis University Budapest. We did not enrol patients who did not receive contrast agent because of severely reduced kidney function (glomerular filtration rate (GFR) <30 ml/min/1.73 m2), did not provide consent, had undergone prior surgical myectomy or percutaneous transluminal septal myocardial ablation, or with persistent ventricular stimulation by an implanted pacemaker.

The CMR and ECG parameteres of HCM patients were compared to a control group of 35 healthy individuals without any known cardiovascular diseases who underwent non-contrast CMR examinations and a standard 12-lead ECG.

### 3.1.4. Prognostic significance of CMR-based markers in patients with HCM

In our clinical follow-up study, 344 HCM patients were enrolled. We excluded patients if there were no available clinical follow-up data (n=146), they did not receive contrast

agent (n=8), or if the strain analysis was not properly feasible (n=3). All together, 187 HCM patients were involved in the study.

The clinical follow-up was based on the medical records and the National Health Insurance Fund of Hungary record database, which includes up-to-date information on the date of deaths. A combined endpoint and an arrhythmia endpoint were analysed. The combined endpoint included all-cause mortality, heart transplantation, and malignant ventricular arrhythmia or appropriate ICD therapy. The arrhythmia endpoint included malignant ventricular arrhythmia and appropriate ICD therapy.

Informed consent was obtained from each patient. Ethical approval was obtained from the Hungarian National Institute of Pharmacy and Nutrition (OGYEI/29174-4/2019), and the studies were performed in accordance with the ethical standards in the 1964 Declaration of Helsinki and its later amendments.

### 3.2. CMR image acquisition protocol

All CMR examinations were conducted with a 1.5 T MR scanner (Achieva, Philips Medical Systems and Magnetom Aera, Siemens Healthcare) using a 5-channel cardiac coil. Retrospectively gated balanced steady-state free precession (bSSFP) cine images were acquired in 2-chamber, 4-chamber and LV outflow tract views. Additionally, short-axis (SA) images with full coverage of the LV were obtained. If no contraindications for contrast agent administration were present, a bolus of 0.15 mmol/kg of the gadolinium-based contrast agent gadobutrol (Gadovist, Bayer-Schering Pharma) was injected at a rate of 2-3 ml/s through an antecubital intravenous line. LGE images were acquired using a segmented inversion recovery sequence with additional phase-sensitive reconstructions in the same views used for the cine images 10-20 minutes after contrast administration. Healthy volunteers did not receive contrast agents because of ethical considerations.

### 3.3. Image analysis

All post-processing analyses were performed using Medis QMass 7.6 or Medis Suite 3.1 software (Medis Medical Imaging Software, Leiden, The Netherlands).

On cine short axis images end-diastolic and end-systolic cardiac phases were identified. The most basal section was required to show≥50% visible myocardial circumference in order to be included. During conventional contouring epi- and endocardial layers were manually traced. Endocardial layer was detected along the compact myocardium resulting that TPM being included in the ventricular cavity. The LV and RV EF, volumes (end-diastolic volume: EDV, end-systolic volume: ESV, stroke volume: SV), and mass (M) were quantified. Parameters corrected for body surface area (BSA) were calculated, yielding EDVi, ESVi, SVi, and Mi, respectively. Maximal EDWT measurements were taken in an SA slice perpendicular to the myocardial center line, excluding trabeculation.

For TB quantification, we used the same end-systolic and end-diastolic phases. A thresholding algorithm (MassK 7.6, Medis, Leiden, The Netherlands) was used to discriminate between chamber blood and myocardium based on their alter signal intensity. The algorithm calculates blood percentage value for each pixels with the previously described equation (77). For the evaluation of TPM, we used the application default 50% thresholding value for both left and right ventricles without manual correction and TPM, TPMi (TPM/BSA), TPM% (TPM/LVM×100) were calculated.

LV strain analysis was performed with the feature-tracking application of the MedisSuite: QStrain module. Endocardial contour detection was manually performed on the three long-axis (LA) and SA cine images on basal, midventricular and apical slices during the end-systolic and end-diastolic phases. Global longitudinal (GLS), circumferential (GCS) and radial (GRS) LV strain parameters were measured. Strain values for the six basal, six midventricular, and five apical segments were averaged to obtain regional longitudinal and circumferential strain values (basal LS, midventricular LS, apical LS, basal CS, midventricular CS, apical CS). The apex-to-base regional LS and CS ratios were calculated as apical LS/basal LS and apical CS/basal CS, respectively. To assess global dyssynchrony, mechanical dispersion (MD) was measured, which was defined as the standard deviation (SD) of the time-to-peak circumferential (MDC) and longitudinal (MDL) strains of the LV segments expressed as percentages of the cardiac cycle. The SDs of the segmental peak LS and CS (SD-LS-Peak and SD-CS-Peak, respectively) were also assessed.

The amount of myocardial fibrosis was quantified on SA LGE images after manual endo- and epicardial contouring at a grayscale threshold of 5 SDs above the mean signal intensity for normal myocardium. Semiautomated quantification of the myocardial fibrosis was visually controlled, and obvious artefacts were corrected.

### 3.4. ECG analysis

A standard 12-lead ECG (25 mm/s and 10 mm/mV) was obtained while patients were in a supine position during quiet respiration. We assessed LVH with the Cornell index (positive score ≥2.8 mV for men and ≥2.0 mV for women), the Sokolow-Lyon index (positive score ≥3.5 mV) and the Romhilt-Estes score (4 for probable LVH and ≥5 for definitive LVH) as described in Introduction section.

Pathological Q-waves were diagnosed if the Q wave was ≥0.04 s in duration or deeper than ¼ of the following R wave in at least two contiguous leads except the aVR lead.

Fragmented QRS was defined as in previous studies (19–21): the presence of an additional R wave (R'), notching of the R wave or notching in the nadir of the S wave in two contiguous leads in patients with a QRS duration <120 ms. In patients with bundle branch block (a QRS duration ≥120 ms), various RsR' patterns were defined as fQRS depending on the presence of >2 R' waves or >2 notches in the R or S waves in two contiguous leads.

The strain pattern was defined as a descending ST-segment depression of ≥1 mm with an inverted asymmetrical T wave opposite to the QRS axis in at least two contiguous leads.

### 3.5. Statistical analysis

The normality of the distribution of the data was investigated with the Shapiro-Wilk or Kolmogorov–Smirnov test. Equality of LV and RV parameters assessed by different evaluation methods was tested with paired samples t-tests. Comparisons between two independent groups were conducted with an independent t-test or Mann-Whitney test, as appropriate. In the case of three or more groups, group characteristics were compared with one-way analysis of variance or the Kruskal-Wallis test, as appropriate. The correlation between continuous variables was calculated with Spearman's correlation

analysis. The sensitivity of the different ECG hypertrophy indices was compared with the McNemar test. Multiple regression analysis was performed to identify ECG predictors of LVM and myocardial fibrosis. Receiver operating characteristic (ROC) curve analysis was performed to analyze the diagnostic accuracy of a parameter and to identify optimal cutoff values. Univariable associations of time variables with mortality were visualized using Kaplan-Meier curves and compared by the log-rank test. The prognostic value of CMR parameters was assessed with univariable and multivariable Cox proportional hazard regression analyses with the enter selection method. Variables with $p<0.05$ in the univariable analysis were selected as candidates for multivariable analysis. Multicollinearity was measured with the variance inflation factor (VIF). Highly correlated predictors (VIF>2.0) were removed from the multivariable model. The interobserver agreement was examined with the intraclass correlation coefficient (ICC score). Differences were considered statistically significant when $p<0.05$. All analyses were performed by using MedCalc software (version 17.9.5).

# 4. Results

## 4.1. Left and right ventricular parameters quantified with conventional and threshold-based methods

The results of this study were published in The International Journal of Cardiovascular Imaging (78).

### 4.1.1. Comparison of conventional and threshold-based methods

Systematic differences were found in CMR parameters evaluated with conventional and threshold-based methods: volumetric values were lower and masses were higher with the TB method in case of all observers. Mean differences between Conv and TB CMR values are shown in ***Table 2***.

LV and RV stroke volumes over all three observers were different using the conventional method [1) High vs. Mid-experienced LVSVi: 51.7 ± 6.5 vs. 54.9 ± 5.9 $p < 0.001$; 2) High vs. Low-experienced LVSVi: 51.7 ± 6.5 vs. 56.4±6.2 $p<0.001$; same difference for RV parameters: 1) RVSVi: 50.0±6.0 vs. 53.8±6.6 $p<0.01$; 2) 50.0±6.0 vs. 52.9±7.0 $p<0.01$]. Equality of LVSVi was excellent with the TB method, and no significant differences were found between observers (High vs. Mid vs. Low-experienced LVSVi: 48.8±5.9 vs. 50.9±5.5 vs. 50.3±5.3).

### 4.1.2. Trabeculation and papillary muscles in left and right ventricles

The average LV-TPM in end-diastolic phase was around one-third of the left ventricular mass in all observers (LV-TPM% of observers: High 30.3 ±3.9%, Mid 30.0 ±4.04%, Low 26.5±4.0%) while TPM in the right ventricle was measured as approximately half of the right ventricular mass (RV-TPM% of observers: High 54.6±6.6%, Mid 48.3±5.8%, Low 47.0±9.4%).

In both the left and right ventricles, the expert reader measured the highest TPMi compared to other observers (LV-TPMi High 22.5±4.9 vs. Mid 19.9±4.7 and vs. Low-experienced 19.4±3.4; RV-TPMi High vs. Mid-experienced 18.2±4.1 vs. 15.8±2.9 $p<0.001$).

DOI:10.14753/SE.2024.2908

***Table 2**: Left and right ventricular parameters with conventional and threshold-based methods. All LV and RV parameters were significantly different: with TB method volumetric values were lower and masses were higher (paired sample t-test *p < 0.001). Abbreviations: Conv – conventional, TB – Threshold-based, SD – standard deviation, LV – left ventricular, RV – right ventricular, EF – ejection fraction, EDV – end-diastolic volume, ESV – end-systolic volume, SV – stroke volume, M – mass, i – index*

| | High-experienced | | | Mid-experienced | | | Low-experienced | | |
|---|---|---|---|---|---|---|---|---|---|
| | Conv Mean±SD | TB Mean±SD | Conv-TB Mean±SD | Conv Mean±SD | TB Mean±SD | Conv-TB Mean±SD | Conv Mean±SD | TB Mean±SD | Conv-TB Mean±SD |
| LVEF (%) | 56.0±4.8 | 66.8±4.8* | −10.8±3.5 | 58.9±4.7 | 68.1±4.7* | −9.2±4.4 | 59.6±5.0 | 68.3±4.9* | −8.7±1.9 |
| LVEDVi ($ml/m^2$) | 92.6±11.0 | 73.3±8.3* | 19.3±4.4 | 93.5±10.6 | 75.0±8.8* | 18.5±3.3 | 94.9±10.8 | 73.8±7.8* | 21.1±4.8 |
| LVESVi ($ml/m^2$) | 41.0±7.5 | 24.4±5.0* | 16.6±4.2 | 38.6±7.3 | 24.1±5.4* | 14.5±3.0 | 38.5±7.5 | 23.6±5.1* | 14.9±3.3 |
| LVSVi ($ml/m^2$) | 51.7±6.5 | 48.8±5.9* | 2.9±3.6 | 54.9±5.9 | 50.9±5.5* | 4.0±2.8 | 56.4±6.2 | 50.3±5.3* | 6.1±2.9 |
| LVMi ($g/m^2$) | 46.1±8.7 | 66.1±11.7* | −20.0±4.6 | 55.1±12.7 | 74.3±14.5* | −19.2 ±3.3 | 50.6±9.4 | 72.8±13.5* | −22.2 ±6.0 |
| RVEF (%) | 54.0±5.2 | 59.3±5.6* | −5.3±2.5 | 57.7±4.1 | 63.2±4.8* | −5.5±2.8 | 56.7±4.7 | 64.2±5.1* | −7.5±2.8 |
| RVEDVi ($ml/m^2$) | 92.6±10.0 | 76.5±9.9* | 16.1±3.2 | 93.5±11.2 | 78.9±11.9* | 14.6±3.3 | 93.7±13.1 | 77.1±11.2* | 16.6±3.9 |
| RVESVi ($ml/m^2$) | 42.7±7.5 | 31.2±6.3* | 11.5±5.7 | 39.7±6.7 | 29.0±5.6* | 10.7±2.5 | 40.8±8.4 | 27.7±6.1* | 13.1±3.3 |
| RVSVi ($ml/m^2$) | 50.0±6.0 | 45.3±6.6* | 4.7±3.1 | 53.8±6.6 | 49.9±8.5* | 3.9±3.7 | 52.9±7.0 | 49.4±7.7* | 3.5±3.0 |
| RVMi ($g/m^2$) | 18.8±4.4 | 35.6±5.3* | −16.8±3.1 | 17.7±6.5 | 33.0±5.7* | −15.3±3.5 | 14.7±3.9 | 32.5±5.8* | −17.8±3.8 |

DOI:10.14753/SE.2024.2908

### 4.1.3. Interobserver reliability of different CMR evaluation methods

Comparing the two methods, interobserver variability of LV parameters was lower using TB analysis and for the evaluation of RV values TB method had superiority against conventional analysis. Global intraclass correlation (G-ICC) value represents interobserver agreement of all investigated LV and RV parameters. However, both G-$ICC_{Conv}$ and G-$ICC_{TB}$ were excellent, G-$ICC_{TB}$ was higher than G-$ICC_{Conv}$ (***Table 3***).

***Table 3****: The intraclass correlation coefficients of conventional and threshold-based methods calculated for LV, RV and all CMR parameters for all observers. Abbreviations: CMR – cardiac magnetic resonance, LV – left ventricular, RV – right ventricular, SD – standard deviation*

| | Conventional<br>Mean±SD | Threshold-based<br>Mean±SD | p |
|---|---|---|---|
| LV CMR parameters | 0.92±0.04 | 0.96±0.03 | p<0.0001 |
| RV CMR parameters | 0.80±0.02 | 0.89±0.08 | p<0.0001 |
| Global CMR parameters | 0.86±0.03 | 0.92±0.02 | p<0.0001 |

Regarding distinct CMR parameters, interobserver agreement was excellent for LV and RV parameters with both methods ***(Table 4)***.

***Table 4****: The intraclass correlation coefficients of conventional and threshold-based methods calculated for each parameter separately. Abbreviations: ICC – intraclass correlation, LV – left ventricular, RV – right ventricular, EF – ejection fraction, EDV – end-diastolic volume, ESV – end-systolic volume, SV – stroke volume, M – mass, i – index*

| | Conventional method | | | Threshold-based method | | |
|---|---|---|---|---|---|---|
| | ICC | 95% confidence interval | | ICC | 95% confidence interval | |
| LVEF | 0.882 | 0.653 | 0.947 | 0.915 | 0.863 | 0.948 |
| LVEDVi | 0.978 | 0.962 | 0.987 | 0.969 | 0.950 | 0.981 |
| LVESVi | 0.959 | 0.914 | 0.978 | 0.956 | 0.932 | 0.973 |
| LVSVi | 0.897 | 0.674 | 0.955 | 0.927 | 0.874 | 0.957 |
| LVMi | 0.868 | 0.604 | 0.942 | 0.936 | 0.738 | 0.975 |
| RVEF | 0.819 | 0.625 | 0.905 | 0.761 | 0.479 | 0.878 |
| RVEDVi | 0.947 | 0.919 | 0.967 | 0.960 | 0.935 | 0.975 |
| RVESVi | 0.910 | 0.849 | 0.947 | 0.897 | 0.779 | 0.946 |
| RVSVi | 0.880 | 0.757 | 0.936 | 0.883 | 0.742 | 0.940 |
| RVMi | 0.748 | 0.537 | 0.858 | 0.920 | 0.801 | 0.961 |

### 4.2. Differential diagnosis of myocardial diseases causing left ventricular hypertrophy

Partial results of this research were published in Plos One (79) and in Cardiologia Hungarica (80).

#### 4.2.1. Patient population

Over a 10-year period, 404 patients were diagnosed with myocardial disease causing LVH or increased LV wall thickness using CMR imaging. The most common diagnosis was HCM, which was detected in 330 patients (82%). CA was diagnosed in 46 patients (11%), FD in 12 patients (3%) and EMF in 16 patients (4%). The most common type of amyloidosis was light chain (AL) amyloidosis (n=35); in one and three patients, serum amyloid A (AA) and transthyretin (TTR) amyloidosis, respectively, were found to have caused CA. In 7 patients, the exact type of amyloidosis was unknown. Among FD patients, the diagnosis was known previously in six cases, and two patients were examined because of a positive family history. Among EMF patients, hypereosinophilic syndrome was previously known in five patients; in four patients, EMF was suggested by echocardiography. CMR imaging provided a different diagnosis from the referral diagnosis for 8% of HCM, 28% of CA, 33% of FD, and 44% of EMF patients.

#### 4.2.2. Conventional CMR parameters

The demographic and CMR data of the patient groups are summarized in ***Table 5***. CA patients were older than the others, and among EMF patients, the percentage of female sex was higher. CA and EMF patients had a lower LVEF and LVSVi than HCM and FD patients. CA patients had a higher LVESVi than HCM patients. EMF patients had a lower LVMi and EDWT than the other groups. CA and EMF patients had higher amounts of LGE than HCM and FD patients.

#### 4.2.3. Feature-tracking strain analysis

CA patients had lower GRS and more impaired global, basal and midventricular LS than the other groups (***Table 5***). Global, basal, midventricular and apical CS were more impaired in CA and EMF patients than in HCM and FD patients. FD patients had a lower MDL and MDC, and HCM patients had a higher SD-LS-Peak, a more negative apical LS

and a higher GRS/EF ratio than the other groups. The apex-to-base CS and LS ratios were the highest in CA and the lowest in EMF patients.

***Table 5***: *Demographic and CMR characteristics of the study population. Comparison of the parameters of patients with different diagnosis. Abbreviations: HCM – hypertrophic cardiomyopathy, CA – cardiac amyloidosis, FD – Fabry disease, EMF – endomyocardial fibrosis, BSA – body surface area, LV – left ventricular, EF – ejection fraction, EDV – end-diastolic volume, ESV – end-systolic volume, SV – stroke volume, M – mass, i – index, EDWT – end-diastolic wall thickness, LGE – late gadolinium enhancement, G – global, R – radial, C – circumferencial, L – londitudinal, S – strain, MD – mechanical dispersion, SD – standard deviation*

| | **HCM (n=330)** | **CA (n=46)** | **FD (n=12)** | **EMF (n=16)** | p |
|---|---|---|---|---|---|
| | median (interquartile range) | median (interquartile range) | median (interquartile range) | median (interquartile range) | |
| age | 48.0 [35.0 to 60.0] | 65.5 [59.0 to 70.0] | 50.5 [40.0 to 61.0] | 43.5 [36.0 to 57.5] | <0.000001 |
| sex (male%) | 61.5 | 63 | 58.3 | 25 | <0.05 |
| BSA ($m^2$) | 1.96 [1.76 to 2.12] | 1.87 [1.65 to 2.01] | 1.82 [1.57 to 2.14] | 1.72 [1.68 to 1.79] | <0.05 |
| LVEF (%) | 64.0 [58.1 to 68.6] | 50.3 [44.6 to 58.4] | 60.0 [56.0 to 70.0] | 60.0 [50.8 to 62.0] | <0.000001 |
| LVEDVi ($ml/m^2$) | 86.0 [75.0 to 95.7] | 78.7 [69.9 to 100.0] | 85.0 [74.5 to 104.5] | 72.0 [64.0 to 94.8] | 0.29 |
| LVESVi ($ml/m^2$) | 30.4 [25.1 to 37.9] | 39.1 [29.2 to 52.6] | 31.5 [23.0 to 43.0] | 31.0 [25.0 to 45.8] | <0.001 |
| LVSVi ($ml/m^2$) | 55.0 [47.0 to 61.8] | 42.0 [35.1 to 49.8] | 53.5 [48.5 to 61.5] | 44.0 [38.0 to 50.3] | <0.000001 |
| LVMi ($g/m^2$) | 83.1 [67.9 to 104.0] | 89.2 [77.0 to 101.4] | 94.5 [70.0 to 128.5] | 53.0 [45.8 to 63.3] | <0.00001 |
| EDWT (mm) | 20.0 [17.0 to 24.0] | 18.0 [16.0 to 19.0] | 17.5 [15.0 to 21.0] | 15.0 [14.0 to 16.8] | <0.000001 |
| LGE% | 5.9 [3.0 to 10.6] | 27.1 [18.7 to 40.1] | 4.9 [3.3 to 10.0] | 18.3 [14.6 to 22.0] | <0.000001 |
| GRS (%) | 86.3 [70.1 to 102.6] | 51.9 [37.2 to 71.9] | 73.6 [59.8 to 92.5] | 63.9 [48.3 to 91.7] | <0.000001 |
| GCS (%) | -41.4 [-46.3 to -36.0] | -32.0 [-39.3 to -26.3] | -40.7 [-42.5 to -37.0] | -33.5 [-37.5 to -29.6] | <0.000001 |
| GLS (%) | -24.3 [-26.8 to -20.9] | -18.4 [-22.6 to -15.4] | -22.6 [-24.8 to -19.7] | -22.5 [-30.1 to -17.5] | <0.000001 |
| SD-LS-Peak | 12.0 [10.4 to 13.8] | 10.5 [8.0 to 12.3] | 10.2 [9.2 to 11.7] | 10.2 [9.2 to 11.7] | <0.0001 |
| MDC (%) | 6.0 [4.1 to 8.9] | 6.6 [4.1 to 8.9] | 4.0 [2.7 to 6.5] | 7.3 [5.9 to 9.1] | <0.05 |
| MDL (%) | 16.3 [12.2 to 20.1] | 18.0 [14.7 to 21.0] | 11.5 [8.1 to 15.6] | 13.1 [10.3 to 19.4] | <0.01 |
| basal CS (%) | -38.0 [-42.4 to -32.6] | -24.2 [-31.5 to -20.1] | -33.5 [-40.2 to -27.9] | -32.0 [-37.9 to -26.1] | <0.001 |
| mid CS (%) | -38.1 [-43.8 to -32.5] | -28.6 [-35.9 to -24.2] | -37.3 [-38.6 to -31.5] | -31.5 [-34.3 to -27.1] | <0.001 |

DOI:10.14753/SE.2024.2908

| | | | | | |
|---|---|---|---|---|---|
| apical CS (%) | -48.5 [-55.8 to -40.4] | -42.2 [-50.8 to -34.1] | -48.5 [-57.6 to -43.2] | -37.1 [-45.3 to -28.4] | <0.001 |
| apex-to-base CS | 1.27 [1.10 to 1.46] | 1.67 [1.30 to 1.89] | 1.42 [1.25 to 1.79] | 1.17 [0.87 to 1.52] | <0.0001 |
| basal LS (%) | -20.9 [-24.7 to -16.9] | -13.8 [-17.1 to -11.8] | -18.1 [-23.0 to -16.9] | -21.7 [-28.4 to -17.9] | <0.000001 |
| mid LS (%) | -23.9 [-30.5 to -19.0] | -17.4 [-23.8 to -13.8] | -25.6 [-31.4 to -20.6] | -24.8 [-32.8 to -20.7] | <0.001 |
| apical LS (%) | -30.7 [-35.8 to -24.9] | -23.7 [30.0 to -20.4] | -24.6 [-29.9 to -21.5] | -24.6 [29.0 to -21.5] | <0.001 |
| apex-to-base LS | 1.47 [1.11 to 1.86] | 1.70 [1.40 to 2.32] | 1.27 [1.04 to 1.73] | 1.08 [0.86 to 1.46] | <0.001 |
| GLS/EF | -0.38 [-0.42 to -0.34] | -0.36 [-0.39 to -0.32] | -0.36 [-0.40 to -0.33] | -0.39 [-0.48 to -0.35] | 0.09 |
| GCS/EF | -0.64 [-0.71 to -0.58] | -0.66 [-0.71 to -0.56] | -0.64 [-0.69 to -0.59] | -0.59 [-0.65 to -0.53] | 0.18 |
| GRS/EF | 1.34 [1.13 to 1.54] | 1.03 [0.85 to 1.21] | 1.19 [1.03 to 1.32] | 1.12 [0.98 to 1.43] | <0.000001 |

### 4.2.4. Differentiation of AL-CA from HCM

In the differentiation of AL-CA and HCM, the amount of LGE, basal CS, basal LS, and GRS had the highest diagnostic accuracies. The results of ROC analyses are shown in ***Table 6***.

***Table 6****: Diagnostic accuracy of CMR parameters in differentiating AL-CA from HCM. Results of the ROC curve analyses. Abbreviations: HCM – hypertrophic cardiomyopathy, CA – cardiac amyloidosis, LV – left ventricular, EF – ejection fraction, ESV – end-systolic volume, SV – stroke volume, LGE – late gadolinium enhancement, i – index, EDWT – end-diastolic wall thickness, G – global, R – radial, C – circumferencial, L – londitudinal, S – strain, MD – mechanical dispersion, SD – standard deviation*

| | AL-CA vs. HCM | | | | |
|---|---|---|---|---|---|
| | sensitivity | specificity | cut off | AUC | p |
| LVEF | 60% | 95% | <53% | 0.829 | <0.001 |
| LVESVi | 60% | 70% | >37 ml/m$^2$ | 0.708 | <0.001 |
| LVSVi | 66% | 87% | <43 ml/m$^2$ | 0.774 | <0.001 |
| max. EDWT | 94% | 41% | <20 mm | 0.634 | <0.001 |
| LGE% | 76% | 87% | >16% | 0.916 | <0.001 |
| GRS | 83% | 70% | <74% | 0.847 | <0.001 |
| GCS | 66% | 75% | >-36% | 0.746 | <0.001 |
| GLS | 86% | 63% | >-23% | 0.803 | <0.001 |
| SD-LS-Peak | 66% | 65% | <11 | 0.671 | <0.001 |
| basal CS | 71% | 83% | >-31% | 0.874 | <0.001 |
| mid CS | 63% | 82% | >-31% | 0.734 | <0.001 |
| apical CS | 71% | 54% | >-47% | 0.653 | <0.01 |
| apex-to-base CS | 63% | 74% | >1.44 | 0.741 | <0.001 |
| basal LS | 69% | 85% | >-16% | 0.847 | <0.001 |
| mid LS | 83% | 43% | >-25% | 0.703 | <0.001 |
| apical LS | 60% | 79% | >-24% | 0.731 | <0.001 |
| apex-to-base LS | 71% | 49% | >1.45 | 0.609 | <0.05 |
| GRS/EF | 83% | 64% | <1.26 | 0.8 | <0.001 |

DOI:10.14753/SE.2024.2908

### 4.2.5. Patient prognoses

During the mean 4.2±2.8 years of follow-up, 21 HCM patients (6%), 29 CA patients (63%), 2 FD patients (17%) and 4 EMF patients (25%) died. HCM patients had the highest survival probability, and CA patients had the lowest survival probability (***Figure 7***).

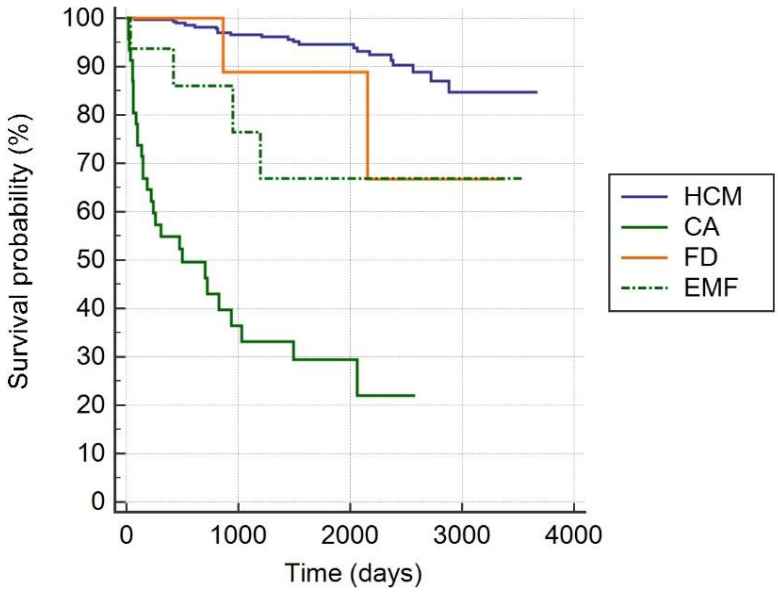


***Figure 7****: Survival probability of patients with different diagnoses (Kaplan-Meier curves). (Source: Figure was not published previously.)*

The results of the univariable and multivariable Cox analyses are summarized in ***Table 7***. Multivariable Cox analysis revealed a diagnosis of CA, LVSVi and basal LS as significant, independent predictors of mortality ($p<0.0001$).

DOI:10.14753/SE.2024.2908

***Table 7**: Predictors of mortality assessed with univariable and multivariable Cox proportional hazard regression analyses. Abbreviations: CA – cardiac amyloidosis, FD – Fabry disease, EMF – endomyocardial fibrosis, BSA – body surface area, LV – left ventricular, EF – ejection fraction, EDV – end-diastolic volume, ESV – end-systolic volume, SV – stroke volume, M – mass, i – index, EDWT – end-diastolic wall thickness, LGE – late gadolinium enhancement, G – global, R – radial, C – circumferencial, L – londitudinal, S – strain, MD – mechanical dispersion, SD – standard deviation*

| | univariate analysis | | multivariate analysis | |
|---|---|---|---|---|
| | p | HR [95% CI] | p | HR [95% CI] |
| CA | <0.0001 | 23.31 [12.88 to 42.18] | <0.05 | 6.73 [1.49 to 30.54] |
| FD | 0.18 | 2.70 [0.63 to 11.53] | 0.74 | 1.47 [0.14 to 15.23] |
| EMF | <0.01 | 4.78 [1.63 to 13.97] | 0.46 | 2.30 [0.26 to 20.52] |
| age | <0.0001 | 1.06 [1.04 to 1.08] | 0.34 | 1.02 [0.98 to 1.05] |
| female | 0.34 | 1.29 [0.76 to 2.18] | | |
| BSA | 0.28 | 0.57 [0.20 to 1.58] | | |
| LVEF | <0.0001 | 0.89 [0.87 to 0.92] | | |
| LVEDVi | 0.68 | 1.00 [0.99 to 1.02] | | |
| LVESVi | <0.0001 | 1.05 [1.03 to 1.06] | | |
| LVSVi | <0.0001 | 0.93 [0.91 to 0.96] | <0.05 | 0.95 [0.91 to 0.99] |
| LVMi | 0.09 | 1.01 [1.00 to 1.01] | | |
| EDWT | <0.05 | 0.94 [0.88 to 0.99] | 0.78 | 0.98 [0.82 to 1.16] |
| LGE% | <0.0001 | 1.05 [1.03 to 1.06] | 0.47 | 0.99 [0.96 to 1.02] |
| GRS | <0.0001 | 0.96 [0.95 to 0.97] | | |
| GCS | <0.0001 | 1.08 [1.05 to 1.11] | | |
| GLS | <0.0001 | 1.11 [1.07 to 1.15] | | |
| SD-LS-Peak | <0.01 | 0.86 [0.78 to 0.96] | | |
| MDC | 0.053 | 1.06 [1.00 to 1.13] | | |
| MDL | <0.01 | 1.07 [1.02 to 1.12] | | |
| basal CS | <0.0001 | 1.12 [1.07 to 1.16] | | |
| mid CS | <0.0001 | 1.08 [1.04 to 1.12] | | |
| apical CS | <0.001 | 1.04 [1.02 to 1.06] | | |
| apex-to-base CS | <0.01 | 2.69 [1.50 to 4.81] | 0.76 | 1.11 [0.57 to 2.17] |
| basal LS | <0.0001 | 1.20 [1.12 to 1.29] | <0.05 | 1.14 [1.02 to 1.28] |
| mid LS | <0.0001 | 1.10 [1.05 to 1.16] | 0.58 | 1.02 [0.95 to 1.10] |
| apical LS | <0.01 | 1.06 [1.02 to 1.10] | 0.84 | 0.99 [0.94 to 1.05] |
| apex-to-base LS | <0.05 | 1.55 [1.02 to 2.36] | | |
| GLS/EF | 0.1 | 12.44 [0.61 to 252.71] | | |
| GCS/EF | 0.35 | 0.30 [0.02 to 3.74] | | |
| GRS/EF | <0.0001 | 0.12 [0.05 to 0.29] | | |

### 4.3. Electrocardiographic predictors of LVH and myocardial fibrosis in HCM

The results of this study were published in the Annals of Noninvasive Electrocardiology (81).

#### 4.3.1. Patient characteristics

We enrolled 146 HCM patients, and a control group of 35 healthy individuals without any known cardiovascular diseases who underwent CMR examinations and a standard 12-lead ECG at the Heart and Vascular Center of Semmelweis University Budapest. There was no difference between HCM patients and the control group in age (mean age of HCM patients: 49, SD: 17; mean age of controls: 44, SD: 8; p=0.07), in the sex ratio (percent males in the HCM group: 60%; in the control group: 54%; p=0.52), and in the BSA (mean BSA of HCM patients: 1.96, SD: 0.26; mean BSA of controls: 1.90, SD: 0.22; p=0.19). The CMR and ECG characteristics of the study population are summarized in ***Table 8***. In the control group, no pathological alterations were found with CMR.

HCM patients had a significantly higher LVM and maximal EDWT than individuals in the control group. All of the investigated ECG alterations occurred significantly more frequently in patients with HCM (***Table 8***).

DOI:10.14753/SE.2024.2908

***Table 8**: CMR and ECG characteristics of the study population. Abbreviations: HCM – hypertrophic cardiomyopathy, CMR – cardiac magnetic resonance, LV – left ventricular, EF – ejection fraction, EDV – end-diastolic volume, ESV – end-systolic volume, SV – stroke volume, M – mass, i – index, ECG – electrocardiography, fQRS – fragmented QRS*

| | **HCM** | | **Control group** | | **p** |
|---|---|---|---|---|---|
| Number of patients | 146 | | 35 | | |
| ***CMR parameters*** | ***Mean±SD*** | | ***Mean±SD*** | | |
| LVEF (%) | 64±7 | | 62±5 | | 0.19 |
| LVESVi (ml/m²) | 31±8 | | 34±13 | | 0.23 |
| LVEDVi (ml/m²) | 84±15 | | 84±11 | | 0.93 |
| LVSVi (ml/m²) | 53±11 | | 52±6 | | 0.53 |
| LVM (g) | 171±67 | | 87±25 | | <0.0001 |
| LVMi (g/m²) | 87±32 | | 46±10 | | <0.0001 |
| Maximal wall thickness (mm) | 20±5 | | 9±2 | | <0.0001 |
| Myocardial fibrosis (g) | 17±22 | | - | | |
| Myocardial fibrosis (%) | 9±10 | | - | | |
| ***ECG parameters*** | ***number*** | ***%*** | ***number*** | ***%*** | |
| Pathological Q waves | 36 | 25 | 0 | 0 | 0.0011 |
| fQRS | 71 | 49 | 6 | 17 | 0.0007 |
| ST depression | 94 | 64 | 0 | 0 | <0.0001 |
| ST elevation | 35 | 24 | 0 | 0 | 0.0013 |
| T wave inversion | 116 | 80 | 1 | 3 | <0.0001 |
| Strain pattern | 74 | 51 | 0 | 0 | <0.0001 |
| Sokolow-Lyon index positivity | 46 | | 1 | | 0.0005 |
| | Sensitivity 32%, specificity 97%, AUC 0.644 | | | | |
| Cornell index positivity | 51 | | 0 | | <0.0001 |
| | Sensitivity 35%, specificity 100%, AUC 0.675 | | | | |
| Romhilt-Estes score ≥ 5 | 90 | | 0 | | <0.0001 |
| | Sensitivity 62%, specificity 100%, AUC 0.808 | | | | |
| Romhilt-Estes score ≥ 4 | 109 | | 1 | | <0.0001 |
| | Sensitivity 75%, specificity 97%, AUC 0.859 | | | | |

### 4.3.2. Diagnostic accuracy of the different ECG hypertrophy criteria

The sensitivity and specificity of the ECG hypertrophy criteria are summarized in ***Table 8***. All three ECG hypertrophy criteria had a high specificity. A total of 126 (86%) HCM patients met at least one of the three investigated ECG hypertrophy criteria. The Sokolow-Lyon index was positive in 46 (32%) patients, and the Cornell index was positive in 51 (35%) patients. The Romhilt-Estes score suggested definitive LVH (a Romhilt-Estes score ≥5) in 90 (62%) patients and probable LVH (a Romhilt-Estes score = 4) in 19 (13%) additional patients. Comparing the sensitivity of the three investigated ECG voltage criteria, the Romhilt-Estes score was the most sensitive (Romhilt-Estes score vs. Sokolow-Lyon index: difference 43.2%, 95% confidence interval 33.7% to 52.6%, p<0.0001; Romhilt-Estes score vs. Cornell index: difference 39.7%, 95% confidence interval 29.6% to 49.9%, p<0.0001). There was no statistically significant difference in the sensitivity of the Sokolow-Lyon index and Cornell index (difference: 3.4%, 95% confidence interval -7.1% to 13.9%, p=0.61).

The LVMi was positively correlated with the Cornell index (p=0.0018; r=0.257), the Sokolow-Lyon index (p<0.0001; r=0.337), and the Romhilt-Estes score (p<0.0001; r=0.410), which had the strongest correlation (***Figure 8***). In a subgroup of 85 patients, LVM was also quantified using threshold-based method in addition to the conventional method. Using threshold-based method for quantification of the LVM, we have found similar correlations (between $LVMi_{TB}$ and the Cornell index $p < 0.05$, $r = 0.24$; the Sokolow-Lyon index $p < 0.05$, $r = 0.23$; the Romhilt-Estes score $p < 0.001$, $r = 0.40$).

### 4.3.3. Effect of fibrosis on the voltage criteria

The amount of fibrosis was negatively correlated with the Cornell index (p=0.015; r=-0.201) and the Sokolow-Lyon index (p=0.0052; r=-0.230). The Romhilt-Estes score was independent of the amount of fibrosis (p=0.757; r=0.026) (***Figure 8***).

DOI:10.14753/SE.2024.2908

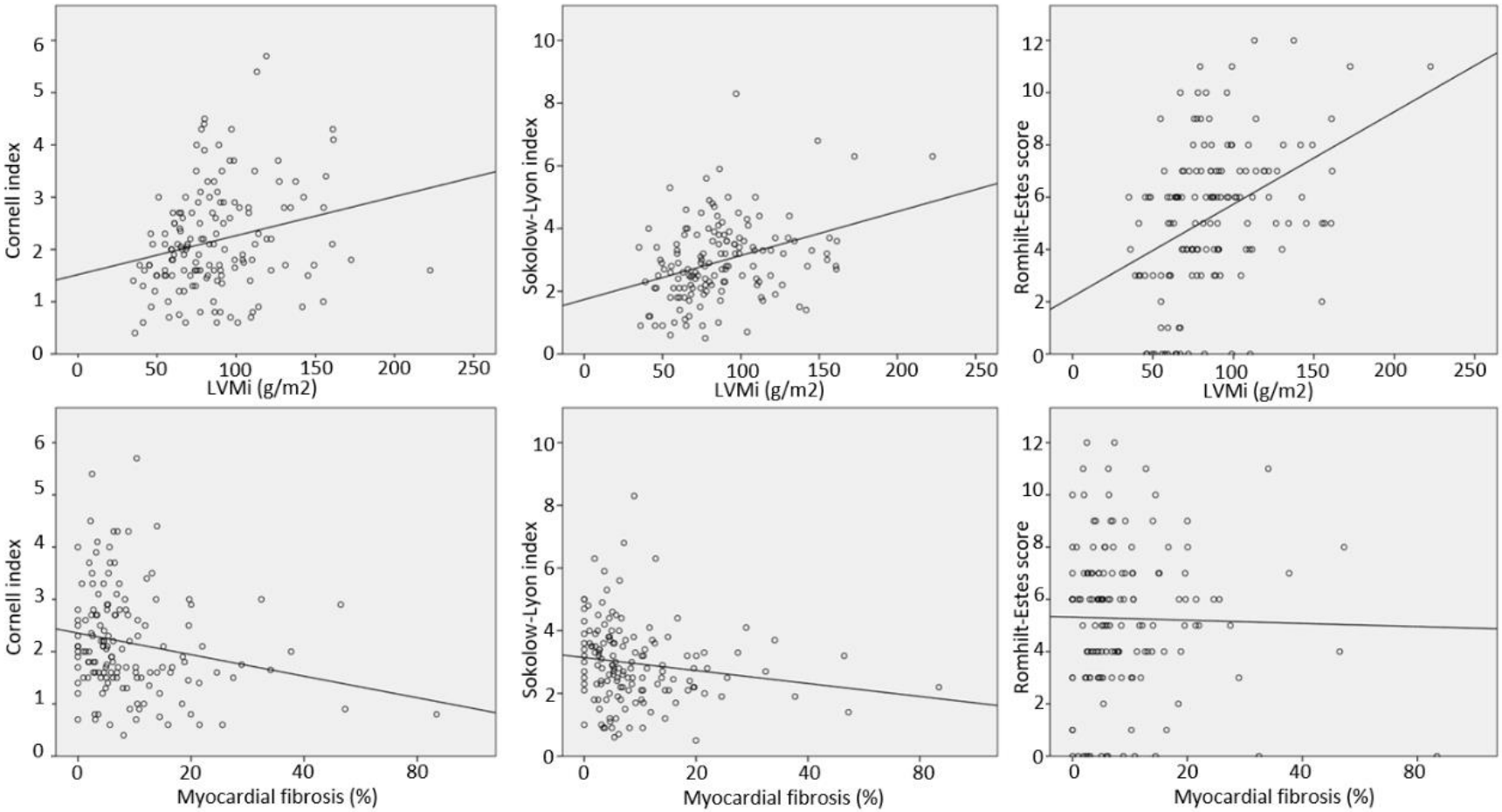


***Figure 8***: *Correlations between the ECG hypertrophy criteria and LVMi, the ECG hypertrophy criteria and myocardial fibrosis (Spearman's correlation). (Source: Figure was published in the Annals of Noninvasive Electrocardiology (81))*

DOI:10.14753/SE.2024.2908

#### 4.3.4. ECG predictors of the LVM and myocardial fibrosis

When we compared the LVM and the amount of fibrosis in HCM patients with and without an ECG abnormality, we found that patients with ST depression, T wave inversion, strain pattern, Sokolow-Lyon index positivity or Romhilt-Estes score positivity had a significantly higher LVM. The amount of myocardial fibrosis was significantly higher in patients with fQRS or strain pattern and was lower in patients with Sokolow-Lyon index positivity. No significant differences in LVM or the amount of myocardial fibrosis were found if a pathological Q wave, ST elevation or Cornell index positivity was present (***Table 9***).

Based on the multivariate analysis, we found that male sex, the strain pattern, the Sokolow-Lyon index and the Romhilt-Estes score were independent positive predictors of LVM ($p<0.0001$). fQRS and the strain pattern predicted more fibrosis, while the Cornell index was a negative predictor of myocardial fibrosis ($p<0.0001$) (***Table 10***).

DOI:10.14753/SE.2024.2908

***Table 9**: Amount of myocardial fibrosis and the LVM in patients with and without an ECG abnormality. Patients with fQRS or strain pattern had more myocardial fibrosis, patients with Sokolow-Lyon index positivity had less myocardial fibrosis. Patients with ST depression, T wave inversion, strain pattern, Sokolow-Lyon index positivity or Romhilt-Estes score positivity had a significantly higher LVM. Abbreviations: ECG – electrocardiography, LVM – left ventricular mass, fQRS – fragmented QRS*

| | ECG abnormality present | | | ECG abnormality absent | | | Fibrosis p | LVM p |
|---|---|---|---|---|---|---|---|---|
| | n | Fibrosis (%) median (interquartile range) | LVM (g) median (interquartile range) | n | Fibrosis (%) median (interquartile range) | LVM (g) median (interquartile range) | | |
| Pathological Q waves | 36 | 7.2 (4.4 to 12.4) | 160 (123 to 225) | 110 | 5.7 (2.6 to 11.7) | 158 (131 to 200) | 0.13 | 0.92 |
| fQRS | 71 | 8.0 (4.4 to 14.5) | 170 (131 to 212) | 75 | 5.0 (2.6 to 8.6) | 152 (120 to 187) | **0.0015** | 0.11 |
| ST depression | 94 | 6.6 (3.2 to 11.2) | 175 (131 to 221) | 52 | 5.2 (2.7 to 13.8) | 145 (115 to 177) | 0.50 | **0.0016** |
| ST elevation | 35 | 5.7 (2.8 to 12.4) | 162 (127 to 191) | 111 | 6.2 (3.4 to 11.1) | 157 (129 to 207) | 0.83 | 0.66 |
| T wave inversion | 116 | 6.2 (3.0 to 12.0) | 162 (131 to 211) | 30 | 6.0 (3.1 to 10.2) | 135 (117 to 182) | 0.87 | **0.0437** |
| Strain pattern | 74 | 6.9 (4.1 to 14.0) | 175 (136 to 223) | 72 | 5.2 (2.4 to 9.7) | 146 (113 to 187) | **0.0174** | **0.0032** |
| Sokolow-Lyon index positivity | 46 | 4.5 (1.9 to 7.1) | 175 (146 to 213) | 100 | 6.9 (3.8 to 14.0) | 149 (118 to 194) | **0.0023** | **0.0273** |
| Cornell index positivity | 51 | 5.4 (2.6 to 8.8) | 174 (139 to 216) | 95 | 6.2 (3.2 to 12.7) | 157 (124 to 194) | 0.24 | 0.16 |
| Romhilt-Estes score ≥ 4 | 109 | 6.3 (3.4 to 12.7) | 174 (138 to 214) | 37 | 5.0 (2.4 to 10.3) | 129 (91 to 153) | 0.20 | **<0.0001** |
| Romhilt-Estes score ≥ 5 | 90 | 6.1 (3.2 to 12.2) | 175 (142 to 217) | 56 | 5.9 (3.0 to 11.0) | 140 (107 to 179) | 0.82 | **0.0002** |

DOI:10.14753/SE.2024.2908

***Table 10**: ECG predictors of the LVM and myocardial fibrosis. The male gender, the presence of strain pattern, a 1-mV increase in the Sokolow-Lyon index, or a one-point increase in the Romhilt-Estes score independently predicted 54, 19, 9 and 5 g increases in the LVM, respectively. The presence of fQRS or strain patterns independently predicted an additional 4.58% and 4.05% of fibrotic area in the myocardium, respectively. A 1-mV increase in the Cornell index predicted a 2.05% decrease in myocardial fibrosis. Abbreviations: ECG – electrocardiography, LVM – left ventricular mass, fQRS – fragmented QRS*

| | ECG predictors of the LVM (g) | | | | ECG predictors of myocardial fibrosis (%) | | | |
|---|---|---|---|---|---|---|---|---|
| | Univariate analysis | | Multivariate analysis | | Univariate analysis | | Multivariate analysis | |
| | Coefficient | p | Coefficient | p | Coefficient | p | Coefficient | p |
| (Constant) | | | 74.46 | | | | 9.26 | |
| Age | -0.82 | **0.016** | | | -0.07 | 0.16 | | |
| Male gender | 61.77 | **<0.0001** | 53.79 | <0.0001 | -0.81 | 0.63 | | |
| Pathological Q waves | 7.57 | 0.56 | | | 0.88 | 0.64 | | |
| fQRS | 21.44 | 0.054 | | | 5.38 | **0.0008** | 4.58 | 0.0032 |
| ST depression | 36.40 | **0.0015** | | | -0.58 | 0.73 | | |
| ST elevation | -11.03 | 0.40 | | | -0.95 | 0.62 | | |
| T wave inversion | 24.72 | 0.07 | | | 1.04 | 0.61 | | |
| Strain pattern | 32.93 | **0.0028** | 19.48 | 0.045 | 3.93 | **0.015** | 4.05 | 0.0095 |
| Sokolow-Lyon index | 14.83 | **0.0005** | 9.28 | 0.014 | -1.20 | 0.058 | | |
| Cornell index | 13.11 | **0.0174** | | | -1.94 | **0.016** | -2.05 | 0.008 |
| Romhilt-Estes score | 8.32 | **<0.0001** | 5.05 | 0.005 | -0.07 | 0.80 | | |

### 4.4. Prognostic significance of CMR-based markers in patients with HCM

The results of this study were published in The International Journal of Cardiovascular Imaging (82).

#### 4.4.1. Patient characteristics

We enrolled 187 HCM patients in the study that investigated the clinical outcome of HCM patients. The demographic and CMR characteristics of the study population are summarized in ***Table 11***. The patients had the following symptoms: syncope (19%), chest pain (41%), dyspnoea (39%), and palpitation (36%). Three patients were examined after aborted SCD.

#### 4.4.2. CMR characteristics

The majority of the study population (147 patients) had normal LVEF (57-77%), two patients had supra-normal LVEF (>77%), 36 patients had mildly reduced LVEF (41-56%), and two patients had moderately reduced LVEF (30-40%). The most common form of HCM was asymmetric hypertrophy with a septal or an anterior distribution, which was found in 161 patients (81.5%). There were 27 (13.5%) patients with apical HCM, 7 (3.5%) patients with concentric HCM and three (1.5%) patients with midventricular HCM. Myocardial fibrosis was detected in 90.6% of patients. More extensive myocardial fibrosis was associated with higher LVMi ($p<0.0001$, $r=0.495$) and higher maximal end-diastolic wall thickness ($p<0.0001$, $r=0.44$). Impaired GLS correlated with a higher LVMi and more extensive myocardial fibrosis. Higher maximal end-diastolic wall thickness correlated with higher MDL, referring to more pronounced global LV dyssynchrony. LVEF did not correlate with LVH or with the amount of myocardial fibrosis (***Figure 9***).

DOI:10.14753/SE.2024.2908

***Table 11**: Demographic and CMR characteristics of the study population. Comparison of the parameters of patients with and without combined or arrhythmia endpoints. Abbreviations: BSA – body surface area, LV – left ventricular, EF – ejection fraction, EDV – end-diastolic volume, ESV – end-systolic volume, SV – stroke volume, M – mass, TPM – trabeculae and papillary muscles, i – index, EDWT – end-diastolic wall thickness, G – global, R – radial, C – circumferencial, L – londitudinal, S – strain, MD – mechanical dispersion, Conv – conventional method, TB – Threshold-based method*

| | combined endpoint | | | arrhythmia endpoint | | |
|---|---|---|---|---|---|---|
| | yes | no | p | yes | no | p |
| Number of patients | 34 | 153 | | 12 | 168 | |
| Male | 13 (38%) | 86 (56%) | 0.06 | 5 (42%) | 92 (55%) | 0.38 |
| Age (y) | 47.8±20.9 | 46.8±17.9 | 0.52 | 36.0±22.0 | 47.4±17.9 | 0.09 |
| BSA ($m^2$) | 1.81±0.26 | 1.91±0.25 | 0.06 | 1.70±0.37 | 1.90±0.25 | 0.07 |
| LVEF (%) | 62.4±6.9 | 62.9±7.7 | 0.74 | 60.2±8.0 | 62.9±7.6 | 0.26 |
| LVESVi ($ml/m^2$) | 34.9±13.4 | 33.2±10.8 | 0.51 | 38.2±16.2 | 33.3±11.0 | 0.24 |
| LVEDVi ($ml/m^2$) | 91.7±26.4 | 88.1±17.0 | 0.65 | 93.8±28.2 | 88.4±18.2 | 0.65 |
| LVSVi ($ml/m^2$) | 56.6±15.5 | 55.4±10.9 | 0.95 | 55.2±14.6 | 55.5±11.7 | 0.67 |
| $LVMi_{conv}$ ($g/m^2$) | 114.9±52.1 | 88.0±31.2 | <0.001 | 126.2±56.5 | 90.4±35.0 | <0.01 |
| $LVMi_{TB}$ ($g/m^2$) | 142.2±67.5 | 113.0±37.4 | <0.01 | 160.8±75.2 | 115.5±42.1 | <0.01 |
| TPMi ($g/m^2$) | 29.0±15.2 | 24.9±8.4 | 0.17 | 34.0±19.7 | 25.1±9.0 | <0.05 |
| EDWT (mm) | 22.2±5.7 | 20.6±5.7 | 0.14 | 23.0±6.0 | 20.9±5.7 | 0.20 |
| Myocardial fibrosis (g) | 20.9±18.6 | 16.6±21.4 | <0.05 | 29.3±22.9 | 16.4±21.0 | <0.05 |
| Myocardial fibrosis (%) | 9.8±7.4 | 8.4±8.9 | 0.12 | 13.1±8.7 | 8.2±8.7 | <0.05 |
| GLS (%) | -21.2±6.2 | -22.9±5.4 | 0.20 | -20.6±6.9 | -22.7±5.4 | 0.27 |
| GCS (%) | -40.3±8.6 | -40.2±7.5 | 0.90 | -39.1±9.0 | -40.0±7.5 | 0.68 |
| GRS (%) | 76.6±22.0 | 83.4±22.5 | 0.11 | 74.8±21.1 | 82.4±22.6 | 0.26 |
| MDL (%) | 17.7±4.6 | 16.4±5.2 | 0.17 | 17.7±5.7 | 16.5±5.1 | 0.44 |
| MDC (%) | 8.5±4.7 | 7.1±3.8 | 0.10 | 9.3±5.0 | 7.2±3.8 | 0.16 |

DOI:10.14753/SE.2024.2908

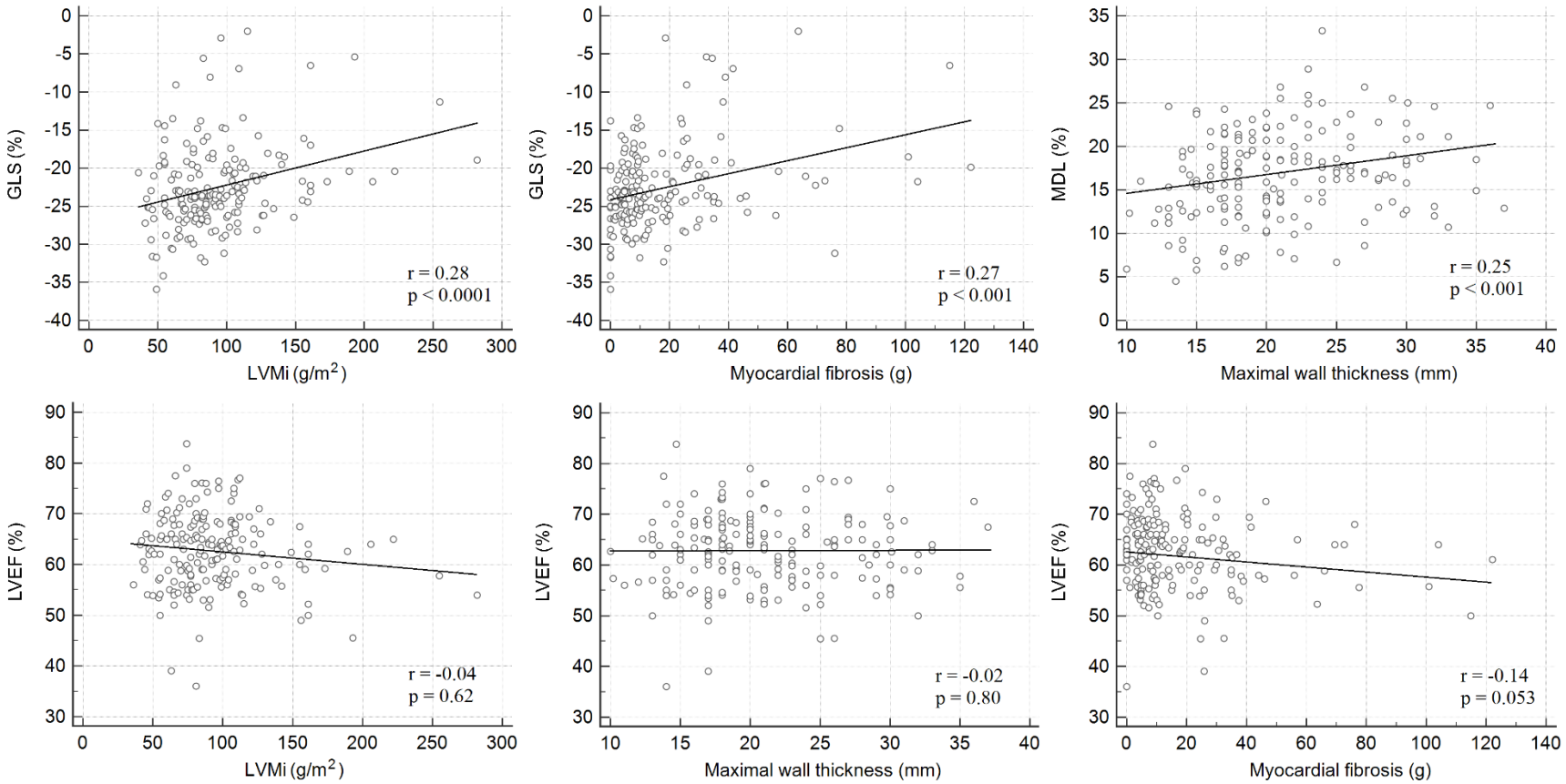


***Figure 9**: Correlation between LV functional parameters and LVH and myocardial fibrosis (Spearman's correlation). (Source: Figure was published in The International Journal of Cardiovascular Imaging (82))*

#### 4.4.3. Clinical outcome

A combined endpoint and an arrhythmia endpoint were analysed. The combined endpoint included all-cause mortality, heart transplantation, and malignant ventricular arrhythmia or appropriate ICD therapy. The arrhythmia endpoint included malignant ventricular arrhythmia and appropriate ICD therapy. During the follow-up (3.8±2.4 years), 20 patients died, and the cause of death was known in 11 patients. One patient died because of brain cancer, cardiovascular death was obvious in 10 cases, and one of them had SCD. In the case of 9 patients, the cause of death was unknown, and these patients were not included in the statistical analyses regarding arrhythmia events. Six patients underwent heart transplantation. One patient had aborted SCD during the follow-up period. ICD implantation occurred in 52 patients (48 as primary prevention), appropriate ICD therapy was detected in 9 patients (6 DC shock, 3 antitachycardia pacing), and one patient had electrical storm. The three patients who were examined after aborted SCD had appropriate ICD therapy during the follow-up.

#### 4.4.4. The prognostic value of CMR

The patients who reached the combined endpoint had higher LVMi both with the conventional and threshold-based evaluation methods. The patients with arrhythmia events had higher $LVMi_{conv}$ and $LVMi_{TB}$, higher TPMi and more extended myocardial fibrosis (***Table 11***).

In the apical HCM group, the endpoint of our study was detected in only one patient who had heart transplantation; however, statistically, there was no difference in the prognosis of the different morphological types of HCM.

$LVMi_{conv}$, $LVMi_{TB}$, GLS, GRS and MDL were significant univariate predictors of the combined endpoint. In the multivariate models, LVMi was an independent predictor of the combined endpoint ($p<0.01$). We investigated the prognostic factors of arrhythmia events, and we found that LVEF, $LVMi_{conv}$, $LVMi_{TB}$, TPMi and myocardial fibrosis were significant univariate predictors of arrhythmia events (***Table 12***).

***Table 12**: Predictors of the combined and arrhythmia endpoints assessed with univariate and multivariate Cox proportional hazard regression analyses. Abbreviations: LV – left ventricular, EF – ejection fraction, EDV – end-diastolic volume, ESV – end-systolic volume, SV – stroke volume, M – mass, TPM – trabeculae and papillary muscles, i – index, EDWT – end-diastolic wall thickness, G – global, R – radial, C – circumferencial, L – londitudinal, S – strain, MD – mechanical dispersion, Conv – conventional method, TB – Threshold-based method*

| | **combined endpoint** | | | | | |
|---|---|---|---|---|---|---|
| | univariate analysis | | multivariate analysis with $LVMi_{Conv}$ | | multivariate analysis with $LVMi_{TB}$ | |
| | p | HR [95% CI] | p | HR [95% CI] | p | HR [95% CI] |
| age | 0.21 | 1.01 [0.99 to 1.03] | | | | |
| female gender | 0.06 | 1.93 [0.97 to 3.87] | | | | |
| LVEDVi | 0.56 | 1.01 [0.99 to 1.02] | | | | |
| LVESVi | 0.13 | 1.02 [0.99 to 1.05] | | | | |
| LVSVi | 0.57 | 0.99 [0.96 to 1.02] | | | | |
| LVEF | 0.051 | 0.95 [0.91 to 1.00] | | | | |
| $LVMi_{Conv}$ | 0.002 | 1.01 [1.003 to 1.02] | 0.011 | 1.01 [1.00 to 1.02] | | |
| $LVMi_{TB}$ | 0.005 | 1.01 [1.002 to 1.01] | | | 0.02 | 1.01 [1.00 to 1.01] |
| TPMi | 0.07 | 1.02 [1.00 to 1.04] | | | | |
| EDWT | 0.90 | 1.004 [0.95 to 1.06] | | | | |
| myocardial fibrosis (%) | 0.42 | 1.01 [0.98 to 1.05] | | | | |
| myocardial fibrosis (g) | 0.51 | 1.005 [0.99 to 1.02] | | | | |
| GLS | 0.02 | 1.08 [1.01 to 1.15] | 0.27 | 1.04 [0.97 to 1.12] | 0.26 | 1.04 [0.97 to 1.12] |
| GCS | 0.81 | 1.01 [1.01 to 1.05] | | | | |
| GRS | 0.048 | 0.98 [0.97 to 0.99] | | | | |
| MDL | 0.048 | 1.07 [1.00 to 1.14] | 0.12 | 1.06 [0.99 to 1.13] | 0.13 | 1.06 [0.98 to 1.13] |
| MDC | 0.06 | 1.08 [0.99 to 1.17] | | | | |
| | **arrhythmia endpoint** | | | | | |
| | univariate analysis | | multivariate analysis with $LVMi_{Conv}$ | | multivariate analysis with $LVMi_{TB}$ | |
| | p | HR [95% CI] | p | HR [95% CI] | p | HR [95% CI] |
| age | 0.19 | 0.98 [0.94 to 1.01] | | | | |
| female gender | 0.34 | 1.76 [0.55 to 5.59] | | | | |
| LVEDVi | 0.54 | 1.01 [0.98 to 1.04] | | | | |
| LVESVi | 0.08 | 1.04 [1.00 to 1.08] | | | | |
| LVSVi | 0.39 | 0.98 [0.93 to 1.03] | | | | |
| LVEF | 0.03 | 0.91 [0.84 to 0.99] | 0.15 | 0.93 [0.84 to 1.03] | 0.13 | 0.92 [0.83 to 1.06] |
| $LVMi_{Conv}$ | 0.01 | 1.01 [1.00 to 1.02] | 0.28 | 1.01 [0.99 to 1.03] | | |
| $LVMi_{TB}$ | 0.009 | 1.01 [1.00 to 1.02] | | | 0.21 | 1.01 [0.99 to 1.03] |
| TPMi | 0.02 | 1.03 [1.00 to 1.06] | 0.71 | 0.99 [0.92 to 1.06] | 0.50 | 0.97 [0.89 to 1.06] |
| EDWT | 0.76 | 1.02 [0.92 to 1.12] | | | | |
| myocardial fibrosis (%) | 0.03 | 1.05 [1.01 to 1.09] | 0.14 | 1.03 [0.99 to 1.08] | 0.15 | 1.03 [0.99 to 1.08] |
| myocardial fibrosis (g) | 0.07 | 1.02 [1.00 to 1.04] | | | | |
| GLS | 0.053 | 1.11 [1.00 to 1.22] | | | | |
| GCS | 0.58 | 1.02 [0.95 to 1.10] | | | | |
| GRS | 0.15 | 0.98 [0.95 to 1.01] | | | | |
| MDL | 0.22 | 1.07 [0.96 to 1.19] | | | | |
| MDC | 0.09 | 1.12 [0.98 to 1.27] | | | | |

DOI:10.14753/SE.2024.2908

Using ROC analysis, we calculated different LVMi cut-offs regarding the combined endpoint: the LVMi cut-off for males with the conventional evaluation method was 108 g/m2, and it was 128 g/m2 with the threshold-based method. The LVMi cut-off for females with the conventional evaluation method was 86 g/m2, and it was 107 g/m2 with the threshold-based method. The patients with an LVMi less than the cut-off value had significantly better prognosis (***Figure 10***).

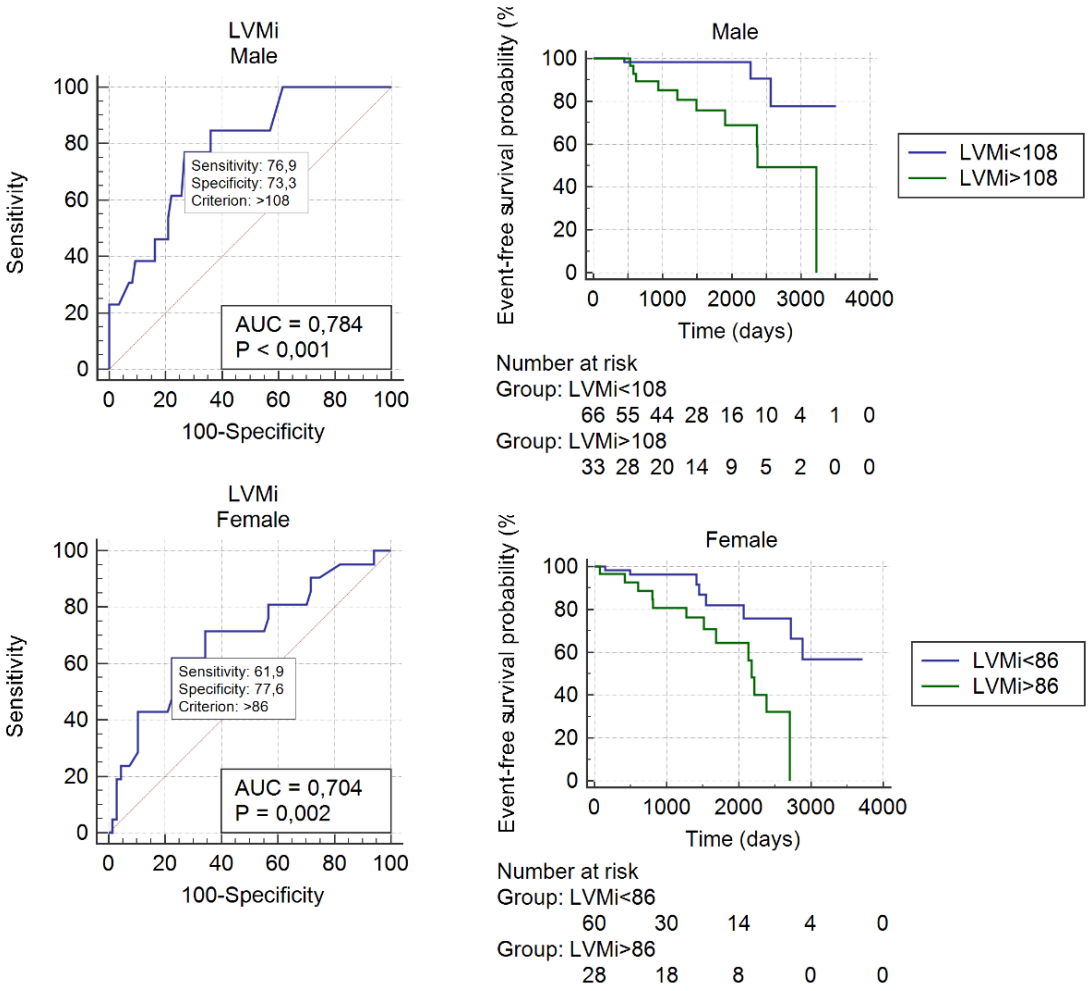


***Figure 10***: *LVMi cut-off for males and females with ROC analysis regarding major events. Event-free survival of patients divided by LVMi cut-off (Kaplan-Meier curves). (Source: Figure was published in The International Journal of Cardiovascular Imaging (82))*

DOI:10.14753/SE.2024.2908

## 5. Discussion

### 5.1. Left and right ventricular parameters corrected with threshold-based method

Quantitative analysis of TPM is controversial, as there is no generally accepted method for the quantification. It is difficult to compare literature data because of the diverse evaluation of TPM volumes. The majority of prior studies presented data that was either papillary muscle or trabecular mass measurement in isolation (77,83–85); few studies are available which reported the sum of papillary and trabecular mass (86–89). Quantitative analysis of TPM could alter normal ventricular values (87,90). Using the TB method, the measured end-diastolic and end-systolic volumes are lower, while the EF end mass are higher compared to the conventional method. Similar results were found in a previous study, although there are differences in the values compared to our study, which may be explained by the different software used (91).

In our study, we compared two different LV and RV measurements focusing on interobserver variability of readers with different experience. We determined the global ICC score for all measured CMR parameters. Although interobserver agreement was excellent for both methods, it was statistically significantly higher for the TB method. The TB- method has improved accuracy comparing aortic flow measurement as a reference (29); accordingly, our data proved excellent equality of left and right ventricular stroke volumes with TB analysis compared to the conventional method.

Left ventricular mass is a widely accepted morphological parameter to assess and predict clinical and cardiovascular outcomes (92,93). Our data regarding the sum of papillary muscle and trabecular mass in the left ventricle was consistent with large population based literature data in all observers (87). In our further studies, where we investigated the use of the TB method in patients with HCM, we found that LVM determined by conventional and TB methods correlated similarly with ECG hypertrophy indices, and that LVM influenced the prognosis of patients independently of the evaluation method.

Although right ventricular morphology and function have a diagnostic and prognostic value in cardiovascular (94–97) and pulmonary diseases (96,98,99), TPM and TPM

corrected RV parameters are not-well understood. Trabeculation in RV significantly affects quantifications of volumes and masses; indeed, in our study ca. half of the right ventricular mass was measured as TPM which is not a negligible fraction.

Threshold-based semi-automatic quantification methods are a user-friendly, accurate and consistent for evaluating LV and RV CMR parameters. Based on our results, the experience of the evaluator did not have any considerable effect on either LV or RV CMR parameters while using the TB quantification method.

Limitations of the study: the limited patient number and the lack of scan-rescan reproducibility. The high differences of ICC values between the conventional and TB methods partially may come from the altering ranges of the measured parameters.

### 5.2. Differential diagnosis of myocardial diseases causing left ventricular hypertrophy

Analyzing a cohort of 330 HCM patients, 46 CA patients, 12 FD patients and 16 EMF patients, our main findings are as follows: 1) CA patients have the highest apex-to-base CS and LS ratios, suggestive of apical sparing. 2) In the differentiation of AL-CA from HCM, the amount of LGE have the highest diagnostic accuracy, followed by basal LS, basal CS and GRS. 3) FD patients have the lowest MDL and MDC, meaning that compared to that of other patients with LVH, global dyssynchrony is least pronounced in this patient population. 4) EMF patients have impaired global, basal, midventricular and apical CS and the lowest apex-to-base CS and LS ratios with respect to the other three groups. 5) CA patients have the worst prognosis, and the significant independent predictors of mortality are a diagnosis of CA, LVSVi and basal LS.

The diagnosis of CA with CMR examination is traditionally based on the LVH phenotype and the pattern of LGE (43,44). In our study population, it was found that the amount of LGE had the highest diagnostic accuracy in the differentiation of AL-CA from HCM. A recent meta-analysis based on 18 published studies included 1,108 CA patients (69% were AL) and 907 control subjects, estimated a sensitivity and specificity of 84% and 80%, respectively, for LGE in diagnosing CA (100). According to another meta-analysis of 7 studies, the sensitivity and specificity of LGE CMR in diagnosing CA were 85% and

92%, respectively (101). Expert consensus recommendations (43,44) state that CMR has a central role in the non-invasive diagnosis of CA referring to several studies in which typical LGE pattern has been shown to have a diagnostic sensitivity of 85% to 90% (47–49,102,103).

However, in case of a contraindication for contrast agent administration, further diagnostic methods are needed. In recent years, novel CMR techniques, such as mapping measurements, have been developed for the quantitative assessment of myocardial changes. CA is characterized by pronouncedly increased native T1 values. In the case of contrast administration, the extracellular volume of the myocardium can be evaluated with T1 mapping. An increase in ECV is an early marker of CA even before the appearance of LGE (50,51). Unfortunately, mapping measurements were not available in our center for the current study.

In the diagnosis of CA, echocardiography-based strain analysis is widely accepted. A well-known typical sign of CA is apical sparing, in which basal LS is severely impaired while apical LS is relatively spared (43,44). However, only a few studies have investigated the CMR-based strain patterns of CA, and the results are controversial. Williams et al. indicated that CA patients have worse GLS than HCM or FD patients, but they found no difference in the apex-to-base LS ratio between CA and HCM patients (104). In another study, CA patients were compared to healthy controls. CA patients had impaired global, basal, midventricular and apical strain values, but no differences were found in the apex-to-base ratios between CA patients and controls; furthermore, the LS values were not different between the apical and basal regions (105). Bhatti et al. investigated multiple myeloma patients with and without CA and found that the apex-to-base gradient was suggestive of apical sparing in patients with CA compared with those without CA, but no differences were found in the CS and RS values (106). Our results demonstrate that feature-tracking strain analysis is applicable for detecting apical sparing in CA patients as they had had significantly higher apex-to-base LS and CS ratios than HCM, FD and EMF patients. However, in the differentiation of AL-CA from HCM, the apex-to-base CS and LS ratios were less accurate than the global and basal strain values.

Limited data are available regarding the CMR-based strain analysis of FD. Previous studies have indicated that FD patients with LVH have more impaired GLS and GCS values than those without LVH (107–110). We did not perform subgroup analysis among FD patients regarding the presence of LVH, as all of the patients had an EDWT of at least 13 mm. In our study, FD patients had similar global strain values to HCM patients; however, we found differences in the dyssynchrony parameters between the two groups. Mechanical dispersion is a reliable parameter for assessing the heterogeneity and global dyssynchrony of LV contraction. Previous studies have indicated that MD, as assessed by echocardiography, could serve as a predictor of ventricular arrhythmias in HCM (111–113). Cianciulli et al. demonstrated that FD patients with LVH have significantly higher MD than those without LVH or healthy controls (114). We found that FD patients had significantly lower MDL and MDC than the other groups, which suggests a more homogenous LV contraction in FD.

To the best of our knowledge, the strain patterns in EMF as assessed by CMR have not been investigated previously. A case report is available on multiparametric CMR imaging, including feature-tracking strain analysis for the diagnosis of EMF, which presented a case of an EMF patient with impaired GLS; however, the GRS, GCS and regional strain values were not described in the report (115). Additionally, limited data are available regarding the echocardiography-based strain characteristics of EMF. Yamamoto et al. investigated patients with hypereosinophilic syndrome and a very early stage of LV endocardial dysfunction and found that hypereosinophilic syndrome patients have impaired GLS; however, GRS, GCS and conventional echocardiographic parameters were similar to those of normal controls (116). In our study, EMF patients had a more impaired GCS value than HCM and FD patients, while GLS was similar to that of HCM or FD patients. The apex-to-base LS and CS ratios were the lowest in this patient population, which is in agreement with the fact that the apical region is the most affected region in EMF.

Amyloidosis is characterized by a progressive clinical course and poor prognosis if the disease is untreated (42–44). Unsurprisingly, CA patients had the lowest survival probability in our study. This result underlines the importance of the proper differential diagnosis of patients with LVH. The prognostic value of feature-tracking strain analysis

has been little investigated in this patient population; in studies that have addressed this topic, impaired global LV strain values were described as predictors of all-cause mortality in HCM and CA patients (35,36). In the current study, the significant independent predictors of mortality were a diagnosis of CA, LVSVi and basal LS.

The limitations of our study include its single-center setting and the relatively low sample size of FD and EMF patient group. The main advantage of feature-tracking strain analysis is that it needs no additional dedicated CMR sequences, and the evaluation is performed using the standard cine images. However, this method has some limitations: previously published data showed that reliability and accuracy of feature-tracking analysis is dependent on reader experience more than tagging-based strain analysis, and the reproducibility of segmental assessment of strain is lower (117–119). Additionally, myocardial T1 and T2 mapping and myocardial extracellular volume measurements were not available. Finally, in the vast majority of HCM patients, no genetic testing was performed, and in 7 CA patients, the exact type of amyloidosis was unknown.

### 5.3. Electrocardiographic predictors of LV hypertrophy and myocardial fibrosis in HCM

The diagnostic value of the different ECG voltage criteria for HCM is mainly investigated using echocardiography (16,120,121). Although CMR is the gold standard noninvasive method for the detection and quantification of myocardial fibrosis, limited data are available regarding the correlation between CMR and ECG characteristics of HCM patients. Hypertrophy and myocardial fibrosis both may have an effect on ECGs, as an increased LVM results in a higher ECG amplitude, but replacement of the myocardium by fibrotic tissue decreases the ECG voltage. Based on the results from the Multi-Ethnic Study of Atherosclerosis (MESA), diffuse myocardial fibrosis was associated with a lower QRS voltage in a large population free of clinical cardiovascular diseases (122). It is also known that end-stage HCM with extensive fibrosis is associated with low voltage on ECGs (70). These studies did not investigate the effect of fibrosis on the Romhilt-Estes score, which is a more complex criterion than the other ECG hypertrophy criteria. In our study, the Romhilt-Estes score was the most sensitive ECG hypertrophy criterion, and this criterion showed the strongest correlation with the LVM. The Romhilt-Estes score was independent of the extent of fibrosis. The explanation that we offer for this finding

is that the Romhilt-Estes score considers not only voltage criteria but also ST-T abnormalities, P-wave features, left axis deviations, QRS durations and delayed intrinsicoid deflections; thus, the complexity of this score may result in a higher diagnostic accuracy in HCM.

Although pathological Q waves are traditionally considered a marker of myocardial scarring, we found no difference in the amount of fibrosis between patients with and without pathological Q waves. In contrast to that result, fQRS and/or strain pattern associated with higher amount of myocardial fibrosis. In previous studies, it was also found that the presence of fQRS might be correlated with more fibrosis (21,69). Other studies that investigated the prognostic significance of fQRS reported that the presence of fQRS was associated with a significant increase in arrhythmic events in HCM patients (123,124). Strain pattern is a known ECG sign of HCM and is associated with a higher cardiovascular risk and abnormal left ventricular function (23,24,125). It is also known that ECG strain is a marker of myocardial fibrosis in aortic stenosis and in hypertension (126,127). To our knowledge, how strain pattern predicts myocardial fibrosis was not previously investigated in patients with HCM. Our results suggest that the presence of fQRS and/or strain pattern indicate a greater amount of myocardial fibrosis in patients with HCM.

fQRS is a relatively common ECG alteration in the normal population. In our control group, 17% of healthy individuals had fQRS. A similar prevalence was found in a Finnish study, and fQRS was present in 19.7% of a middle-aged general population consisting of 10,904 subjects. In this study, the prognostic significance of fQRS was investigated, and the researchers found that fQRS was not associated with increased mortality in subjects without a known cardiac disease (128).

A limitation of our study is that it was a single-centre study with a relatively small control group. As non-contrast CMR examinations were performed in the control group because of ethical considerations, the presence of myocardial fibrosis was unknown in this healthy study population. Myocardial T1 and T2 mapping and myocardial extracellular volume evaluations were not available at the time of the study. Another limitation is that there

was no follow-up of the patients in this study, and no genetic testing was performed in the vast majority of HCM patients.

### 5.4. Prognostic significance of CMR-based markers in patients with HCM

The main findings of our study that investigated the clinical outcome of HCM patients are as follows: 1) LVMi was an independent CMR predictor of major events (mortality, heart transplantation, malignant ventricular arrhythmia or appropriate ICD therapy) independent of the LVMi quantification method. 2) The univariate predictors of major events were LVMi, GLS, GRS and MDL. The univariate predictors of arrhythmia events were LVEF, LVMi, TPMi and myocardial fibrosis. 3) More pronounced LVH was associated with impaired GLS and increased MDL. More extended myocardial fibrosis correlated with impaired GLS. However, LVEF showed no correlation with the degree of LVH or with the extent of myocardial fibrosis.

Several studies have demonstrated that patients with more extensive myocardial fibrosis have a higher risk for malignant ventricular arrhythmias (73,74,129,130). These findings are confirmed by guidelines published since our study, in which LGE above 15% of LVM is considered a high risk of SCD (8,65). Our results are consistent with the supposition of the prognostic role of myocardial fibrosis; in our patient population, myocardial fibrosis was a univariate predictor of malignant ventricular arrhythmias.

Conventionally, maximal EDWT is used to describe LVH and to estimate SCD risk in HCM (131–133). However, data in the literature regarding the prognostic significance of EDWT have been controversial (134). LVM is a more robust measure of the total burden of LVH than a single measurement of the EDWT. A previous study stated that the EDWT does not reflect the degree of LVH in patients with HCM, as patients with the same wall thickness may have substantial differences in LVM (135). In an other study it was found that markedly increased LVMi was more sensitive in predicting outcome, whereas EDWT >30 mm was more specific in HCM patients (136). CMR examination provides the most accurate and reproducible information about LVM, as CMR-based LVM measurements are free of cardiac geometric assumptions (137). We found that higher LVMi predicted poor clinical outcome independent of the evaluation method; nevertheless, the LVMi cut-

off values regarding major events depended on the evaluation method and sex. In our patient population, EDWT was not a predictor of major events.

Myocardial strain analyses provide accurate information about global and regional LV function. Strain by speckle tracking echocardiography has been increasingly applied as a sensitive and early marker of LV dysfunction in different cardiomyopathies. Previous studies have demonstrated the relation of echocardiography-based strain parameters to structural alterations and clinical outcomes in patients with HCM (111,138,139). In a previous study it was investigated in 74 HCM patients, how global strain parameters assessed with FT-CMR effect the patients' prognosis. They found that impaired global LV strain values were associated with all-cause mortality and heart failure events (75). MD was not investigated in their study; however, a previous study demonstrated the prognostic role of MD evaluated with FT-CMR in patients after ST-segment elevation myocardial infarction (140). In our study, GLS, GRS and MDL were univariate predictors of major events. In patients with more pronounced LVH, we found increased global LV dyssynchrony and impaired longitudinal contraction, while LVEF did not correlate with the degree of hypertrophy. These results suggested that the FT strain analysis provides important additional information for the detection of LV dysfunction and for risk stratification in HCM patients.

The limitations of our study are that it was a single-centre study, which might limit the generalizability of our conclusions. Although our study was designed to represent a real-world population, due to the retrospective nature of the study, limited clinical data were available for some patients; therefore, these patients were excluded from the analyses. Myocardial T1 and T2 mapping and myocardial extracellular volume evaluation were not available. In the vast majority of the patients, no genetic testing was performed.

## 6. Conclusion

The precise and standard measurement of LV nad RV CMR parameters is crucial and plays a major role during patient follow-up. Our study highlights the necessity of a consistent method for evaluation of TPM in ventricles to uniform normal CMR values, and to avoid misinterpretation of various methods and inaccurate clinical decision-making. Using the TB method, TPM is automatically detected by the software and added to the myocardial mass. TB method showed higher interobserver agreement than conventional method regardless of the readers' experience.

The treatment and prognosis of different myocardial diseases with LVH varies, which makes accurate differential diagnosis of hypertrophy phenocopies of high importance. Our results show that myocardial diseases with LVH have remarkable differences in CMR characteristics including strain parameters which can be helpful in the differential diagnosis of these conditions. Furthermore, CMR including strain measurement provides additional information for the assessment of prognosis in this patient population.

Investigating the ECG characteristics of HCM, we found that both the degree of LVH and the extent of myocardial fibrosis have an effect on the ECG pattern. Our results suggest that the Romhilt-Estes score detects LVH with the highest sensitivity, as myocardial fibrosis has no effect on this criterion. In contrast to pathological Q waves, fQRS and strain pattern are reliable predictors of myocardial fibrosis.

During clinical follow-up of HCM patinets, we found that LVMi is an independent CMR predictor of major events independently of evaluation method; nevertheless, the LVMi cut-off values regarding major events depended on the evaluation method and sex. In line with previous literature data, our results show that myocardial fibrosis predicts arrhythmia events in HCM patients. Furthermore, CMR-based strain analysis provides additional information for the detection of LV dysfunction and for risk stratification in this patient population.

DOI:10.14753/SE.2024.2908

## 7. Summary

Pathological left ventricular hypertrophy (LVH) can be caused by different factors, including pressure overload, various infiltrative diseases or a primary structural abnormality of the myocardium. The treatment and clinical course of these pathologies vary, so accurate diagnosis is of paramount importance. Cardiac magnetic resonance (CMR) imaging is a non-invasive reference method for cardiac morphology, function and myocardial tissue characterisation, and is becoming increasingly accurate in diagnosis thanks to dynamic developments.

In our study, we investigated the role of conventional CMR parameters, CMR-based strain analysis and the quantification of contrast enhancement indicative of myocardial fibrosis in the differential diagnosis and prognostic assessment, as well as the correlation between ECG and CMR features. We investigated the effect of quantification of trabeculae and papillary muscles (TPM). By conventional evaluation, TPM is part of the ventricular cavity, while by threshold-based method it is part of the myocardium. Our results show that the method of evaluation significantly influences the obtained parameters. We found characteristic differences in the CMR appearance of hypertrophic cardiomyopathy (HCM), amyloidosis (CA), Fabry disease and endomyocardial fibrosis. Our results suggest that CMR-based strain analysis is suitable for detecting apical sparing characteristic of CA described by echocardiography, however, basal and global strain values showed higher diagnostic accuracy in differentiating CA from HCM. CA patients had the worst prognosis, the significant independent predictors of mortality were a diagnosis of CA, LVSVi and basal LS. Examining the ECG characteristics of HCM, we found significant differences in the sensitivity of the hypertrophy ECG criteria, with the Romhilt-Estes score having the highest diagnostic value. This criterion was independent of the amount of myocardial fibrosis, while the value of the criteria based on QRS amplitude alone decreased with increasing amount of fibrosis. Fragmented QRS and ECG strain pattern were shown to be predictive of myocardial fibrosis. When examining the prognosis of patients with HCM, we found that left ventricular mass was an independent predictor of major events (mortality, heart transplantation, malignant arrhythmia), which was not influenced by the evaluation method of left ventricular mass. The amount of myocardial fibrosis had an effect on arrhythmia events.

DOI:10.14753/SE.2024.2908

## 8. Összefoglalás

Kóros bal kamra hypertrophia (BKH) hátterében számos tényező állhat, okozhatja nyomásterhelés, különböző infiltratív betegségek, illetve a szívizom elsődleges strukturális rendellenessége. Ezen kórképek kezelése és klinikai lefolyása eltérő, ezért a pontos diagnózis felállításának kiemelt szerepe van. A szív mágneses rezonanciás (MR) vizsgálat a szív morfológiájának, funkciójának és a szívizom szöveti jellemzésének noninvazív referenciamódszere, a dinamikus fejlődésnek köszönhetően egyre pontosabb diagnózisalkotást tesz lehetővé.

Kutatásunkban vizsgáltuk a hagyományos szív MR paraméterek mellett a strain analízis és a miokardiális fibrózist jelző kontraszthalmozás kvantifikálásának szerepét a differenciáldiagnózisban és a prognózis megítélésében, továbbá az EKG és MR jellegzetességek közötti összefüggéseket. Vizsgáltuk a trabekulák és papilláris izmok (TPM) kvantifikálásának hatását. Hagyományos kiértékeléssel a TPM a kamrai üreg, míg threshold-based módszerrel a szívizom része. Eredményeink alapján a kiértékelés módja szignifikánsan befolyásolja a kapott értékeket. Jellegzetes különbségeket találtunk hypertrophiás cardiomyopathia (HCM), amyloidosis (CA), Fabry-kór és endomiokardiális fibrózis MR megjelenésében. Eredményeink alapján MR vizsgálattal végzett strain analízis alkalmas az echocardiographiával leírt CA-ra jellemző ‘apical sparing’ kimutatására, azonban a CA HCM-től történő differenciálásában a bazális és globális strain értékek magasabb diagnosztikus pontosságot mutattak. A CA betegek prognózisa volt a legrosszabb, a halálozás független prediktorai a CA diagnózisa, a bal kamrai verővolumen és a bazális longitudinális strain voltak. A HCM EKG jellegzetességeit vizsgálva jelentős különbségeket találtunk a hypertrophia EKG kritériumok szenzitivitásában, a Romhilt-Estes score diagnosztikus értéke volt a legmagasabb, ez a kritérium független volt a miokardiális fibrózis mennyiségétől, míg a kizárólag QRS amplitúdón alapuló kritériumok értéke a fibrózis mennyiségének növekedésével csökkent. A fragmentált QRS és az EKG strain jel a miokardiális fibrózis prediktorának bizonyult. A HCM-es betegek prognózisát vizsgálva megállapítottuk, hogy a bal kamrai izomtömeg a major események (halálozás, szívtranszplantáció, malignus aritmia) független prediktora, amit nem befolyásolt az izomtömeg meghatározásának módja. A miokardiális fibrózis mennyisége az aritmia eseményekre volt hatással.

## 9. References

1. Oakley CM. Report of the WHO/ISFC task force on the definition and classification of cardiomyopathies. Br Heart J. 1980;44(6):672–3.

2. Maron BJ, Towbin JA, Thiene G, Antzelevitch C, Corrado D, Arnett D, Moss AJ, Seidman CE, Young JB. Contemporary definitions and classification of the cardiomyopathies: An American Heart Association Scientific Statement from the Council on Clinical Cardiology, Heart Failure and Transplantation Committee; Quality of Care and Outcomes Research and Functio. Circulation. 2006;113(14):1807–16.

3. Arbustini E, Narula N, Dec GW, Reddy KS, Greenberg B, Kushwaha S, Marwick T, Pinney S, Bellazzi R, Favalli V, Kramer C, Roberts R, Zoghbi WA, Bonow R, Tavazzi L, Fuster V, Narula J. The MOGE(S) classification for a phenotype-genotype nomenclature of cardiomyopathy: Endorsed by the world heart federation. J Am Coll Cardiol. 2013;62(22):2046–72.

4. Elliott P, Andersson B, Arbustini E, Bilinska Z, Cecchi F, Charron P, Dubourg O, Kühl U, Maisch B, McKenna WJ, Monserrat L, Pankuweit S, Rapezzi C, Seferovic P, Tavazzi L, Keren A. Classification of the cardiomyopathies: A position statement from the european society of cardiology working group on myocardial and pericardial diseases. Eur Heart J. 2008;29(2):270–6.

5. Elliott PM, Anastasakis A, Borger MA, Borggrefe M, Cecchi F, Charron P, Hagege AA, Lafont A, Limongelli G, Mahrholdt H, McKnna WJ, Mogensen J, Nihoyannopoulos P, Nistri S, Pieper PG, Pieske B, Rapezzi C, Rutten FH, Tillmanns C, Watkins H. 2014 ESC guidelines on diagnosis and management of hypertrophic cardiomyopathy: The task force for the diagnosis and management of hypertrophic cardiomyopathy of the European Society of Cardiology (ESC). Eur Heart J. 2014;35(39):2733–79.

6. Marian AJ, Braunwald E. Hypertrophic cardiomyopathy: Genetics, pathogenesis, clinical manifestations, diagnosis, and therapy. Circ Res. 2017;121(7):749–70.

7. Roma-Rodrigues C, Fernandes AR. Genetics of hypertrophic cardiomyopathy: Advances and pitfalls in molecular diagnosis and therapy. Appl Clin Genet. 2014;7:195–208.

8. Ommen SR, Mital S, Burke MA, Day SM, Deswal A, Elliott P, Evanovich LL, Hung J, Joglar JA, Kantor P, Kimmelstiel C, Kittleson M, Link MS, Maron MS, Martinez MW, Miyake CY, Schaff HV, Semsarian C, Sorajja P. 2020 AHA/ACC Guideline for the Diagnosis and Treatment of Patients With Hypertrophic Cardiomyopathy: A Report of the American College of Cardiology/American Heart Association Joint Committee on Clinical Practice Guidelines. J Am Coll Cardiol. 2020;76(25):e159–240.

9. Wigle ED. The diagnosis of hypertrophic cardiomyopathy. Heart. 2001;709–14.

10. Hancock EW, Deal BJ, Mirvis DM, Okin P, Kligfield P, Gettes LS. AHA/ACCF/HRS Recommendations for the Standardization and Interpretation of the Electrocardiogram. Part V: Electrocardiogram Changes Associated With Cardiac Chamber Hypertrophy A Scientific Statement From the American Heart Association Electrocardiography . J Am Coll Cardiol. 2009;53(11):992–1002.

11. Sokolow M, Lyon TP. The ventricular complex in left ventricular hypertrophy as obtained by unipolar precordial and limb leads. Am Heart J. 1949;37(2):161–86.

12. Casale PN, Devereux RB, Kligfield P, Eisenberg RR, Miller DH, Chaudhary BS, Phillips MC. Electrocardiographic detection of left ventricular hypertrophy: Development and prospective validation of improved criteria. J Am Coll Cardiol. 1985;6(3):572–80.

13. Romhilt DW, Estes EH. A point-score system for the ECG diagnosis of left ventricular hypertrophy. Am Heart J. 1968;75(6):752–8.

14. Charron P, Forissier JF, Amara ME, Dubourg O, Desnos M, Bouhour JB, Isnard R, Hagege A, Bénaiche A, Richard P, Schwartz K, Komajda M. Accuracy of European diagnostic criteria for familial hypertrophic cardiomyopathy in a genotyped population. Int J Cardiol. 2003;90(1):33–8.

15. Delcrè SDL, Di Donna P, Leuzzi S, Miceli S, Bisi M, Scaglione M, Caponi D, Conte MR, Cecchi F, Olivotto I, Gaita F. Relationship of ECG findings to phenotypic expression in patients with hypertrophic cardiomyopathy: A cardiac magnetic resonance study. Int J Cardiol. 2013;167(3):1038–45.

16. Erice B, Romero C, Andériz M, Gorostiaga E, Izquierdo M, Ibáñez J. Diagnostic value of different electrocardiographic voltage criteria for hypertrophic cardiomyopathy in young people. Scand J Med Sci Sport. 2009;19(3):356–63.

17. Varnava AM, Elliott PM, Sharma S, McKenna WJ, Davies MJ. Hypertrophic cardiomyopathy: The interrelation of disarray, fibrosis and small vessel disease. Heart. 2000;84(5):476–82.

18. Fronza M, Raineri C, Valentini A, Bassi EM, Scelsi L, Buscemi ML, Turco A, Castelli G, Ghio S, Visconti LO. Relationship between electrocardiographic findings and Cardiac Magnetic Resonance phenotypes in patients with Hypertrophic Cardiomyopathy. IJC Hear Vasc. 2016;11:7–11.

19. Das MK, Khan B, Jacob S, Kumar A, Mahenthiran J. Significance of a fragmented QRS complex versus a Q wave in patients with coronary artery disease. Circulation. 2006;113(21):2495–501.

20. Pietrasik G, Zareba W. QRS fragmentation: Diagnostic and prognostic significance. Cardiol J. 2012;19(2):114–21.

21. Konno T, Hayashi K, Fujino N, Oka R, Nomura A, Nagata Y, Hodatsu A, Sakata K, Furusho H, Takamura M, Nakamura H, Kawashiri MA, Yamagishi M. Electrocardiographic QRS Fragmentation as a Marker for Myocardial Fibrosis in Hypertrophic Cardiomyopathy. J Cardiovasc Electrophysiol. 2015;26(10):1081–7.

22. Rapezzi C, Arbustini E, Caforio ALP, Charron P, Gimeno-Blanes J, Heliö T, Linhart A, Mogensen J, Pinto Y, Ristic A, Seggewiss H, Sinagra G, Tavazzi L, Elliott PM. Diagnostic work-up in cardiomyopathies: Bridging the gap between clinical phenotypes and final diagnosis. A position statement from the ESC Working Group on Myocardial and Pericardial Diseases. Eur Heart J.

2013;34(19):1448–58.

23. Goldberger AL. Q wave T wave vector discordance in hypertrophic cardiomyopathy: Septal hypertrophy and strain pattern. Br Heart J. 1979;42(2):201–4.

24. Ogah OS, Oladapo OO, Adebiyi AA, Adebayo AK, Aje A, Ojji DB, Salako BL, Falase AO. Electrocardiographic left ventricular hypertrophy with strain pattern: Prevalence, mechanisms and prognostic implications. Cardiovasc J Afr. 2008;19(1):39–45.

25. Hughes RK, Knott KD, Malcolmson J, Augusto JB, Mohiddin SA, Kellman P, Moon JC, Captur G. Apical hypertrophic cardiomyopathy: The variant less known. J Am Heart Assoc. 2020;9(5):1–11.

26. Farber NJ, Reddy ST, Doyle M, Rayarao G, Thompson D V., Olson P, Glass J, Williams RB, Yamrozik JA, Murali S, Biederman RWW. Ex vivo cardiovascular magnetic resonance measurements of right and left ventricular mass compared with direct mass measurement in excised hearts after transplantation: A first human SSFP comparison. J Cardiovasc Magn Reson. 2014;16(1):1–9.

27. Moon JCC, Lorenz CH, Francis JM, Smith GC, Pennell DJ. Breath-hold FLASH and FISP cardiovascular MR imaging: left ventricular volume differences and reproducibility. 2002;(11):789–97.

28. Fieno DS, Jaffe WC, Simonetti OP, Judd RM, Finn JP. TrueFISP: Assessment of accuracy for measurement of left ventricular mass in an animal model. J Magn Reson Imaging. 2002;15(5):526–31.

29. Varga-Szemes A, Muscogiuri G, Schoepf UJ, Wichmann JL, Suranyi P, De Cecco CN, Cannao PM, Renker M, Mangold S, Fox MA, Ruzsics B. Clinical feasibility of a myocardial signal intensity threshold-based semi-automated cardiac magnetic resonance segmentation method. Eur Radiol. 2016;26(5):1503–11.

30. Gommans DHF, Bakker J, Cramer GE, Verheugt FWA, Brouwer MA, Kofflard

MJM. Impact of the papillary muscles on cardiac magnetic resonance image analysis of important left ventricular parameters in hypertrophic cardiomyopathy. Netherlands Hear J. 2016;24(5):326–31.

31. Schnell F, Matelot D, Daudin M, Kervio G, Mabo P, Carré F, Donald E. Mechanical Dispersion by Strain Echocardiography: A Novel Tool to Diagnose Hypertrophic Cardiomyopathy in Athletes. J Am Soc Echocardiogr. 2017;30(3):251–61.

32. Pedrizzetti G, Claus P, Kilner PJ, Nagel E. Principles of cardiovascular magnetic resonance feature tracking and echocardiographic speckle tracking for informed clinical use. J Cardiovasc Magn Reson. 2016;18(1):1–12.

33. Andre F, Steen H, Matheis P, Westkott M, Breuninger K, Sander Y, Kammerer R, Galuschky C, Giannitsis E, Korosoglou G, Katus HA, Buss SJ. Age- and gender-related normal left ventricular deformation assessed by cardiovascular magnetic resonance feature tracking. J Cardiovasc Magn Reson. 2015;17(1):1–14.

34. Schuster A, Hor KN, Kowallick JT, Beerbaum P, Kutty S. Cardiovascular Magnetic Resonance Myocardial Feature Tracking: Concepts and Clinical Applications. Circ Cardiovasc Imaging. 2016;9(4):1–9.

35. Moravsky G, Ofek E, Rakowski H, Butany J, Williams L, Ralph-Edwards A, Wintersperger BJ, Crean A. Myocardial fibrosis in hypertrophic cardiomyopathy: Accurate reflection of histopathological findings by CMR. JACC Cardiovasc Imaging. 2013;6(5):587–96.

36. Messroghli DR, Moon JC, Ferreira VM, Grosse-Wortmann L, He T, Kellman P, Mascherbauer J, Nezafat R, Salerno M, Schelbert EB, Taylor AJ, Thompson R, Ugander M, van Heeswijk RB, Friedrich MG. Clinical recommendations for cardiovascular magnetic resonance mapping of T1, T2, T2 and extracellular volume: A consensus statement by the Society for Cardiovascular Magnetic Resonance (SCMR) endorsed by the European Association for Cardiovascular Imagin (EACVI). J Cardiovasc Magn Reson. 2017;19(1):1–24.

37. Maron BJ, Maron MS, Semsarian C. Genetics of hypertrophic cardiomyopathy after 20 years: Clinical perspectives. J Am Coll Cardiol. 2012;60(8):705–15.

38. Ho CY, Day SM, Ashley EA, Michels M, Pereira AC, Jacoby D, Cirino AL, Fox JC, Lakdawala NK, Ware JS, Caleshu CA, Helms AS, Colan SD, Girolami F, Cecchi F, Seidman CE, Sajeev G, Signorovitch J, Green EM, Olivotto I. Genotype and lifetime burden of disease in hypertrophic cardiomyopathy insights from the sarcomeric human cardiomyopathy registry (SHaRe). Circulation. 2018;138(14):1387–98.

39. Rodrigues JCL, Rohan S, Ghosh Dastidar A, Harries I, Lawton CB, Ratcliffe LE, Burchell AE, Hart EC, Hamilton MCK, Paton JFR, Nightingale AK, Manghat NE. Hypertensive heart disease versus hypertrophic cardiomyopathy: multi-parametric cardiovascular magnetic resonance discriminators when end-diastolic wall thickness ≥ 15 mm. Eur Radiol. 2017;27(3):1125–35.

40. Rader F, Sachdev E, Arsanjani R, Siegel RJ. Left ventricular hypertrophy in valvular aortic stenosis: mechanisms and clinical implications. Am J Med. 2015 Apr;128(4):344–52.

41. Csecs I, Czimbalmos C, Toth A, Dohy Z, Suhai IF, Szabo L, Kovacs A, Lakatos B, Sydo N, Kheirkhahan M, Peritz D, Kiss O, Merkely B, Vago H. The impact of sex, age and training on biventricular cardiac adaptation in healthy adult and adolescent athletes: Cardiac magnetic resonance imaging study. Eur J Prev Cardiol. 2020;27(5):540–9.

42. Wechalekar AD, Gillmore JD, Hawkins PN. Systemic amyloidosis. Lancet. 2016;387(10038):2641–54.

43. Dorbala S, Ando Y, Bokhari S, Dispenzieri A, Falk RH, Ferrari VA, Fontana M, Gheysens O, Gillmore JD, Glaudemans AWJM, Hanna MA, Hazenberg BPC, Kristen AV, Kwong RY, Maurer MS, Merlini G, Miller EJ, Moon JC, Murthy VL, Quarta CC, Rapezzi C, Ruberg FL, Shah SJ, Slart RHJA, Verberne HJ, Bourque JM. ASNC/AHA/ASE/EANM/HFSA/ISA/SCMR/SNMMI expert consensus

recommendations for multimodality imaging in cardiac amyloidosis: Part 1 of 2—evidence base and standardized methods of imaging. J Nucl Cardiol. 2019;26(6):2065–123.

44. Dorbala S, Ando Y, Bokhari S, Dispenzieri A, Falk RH, Ferrari VA, Fontana M, Gheysens O, Gillmore JD, Glaudemans AWJM, Hanna MA, Hazenberg BPC, Kristen AV, Kwong RY, Maurer MS, Merlini G, Miller EJ, Moon JC, Murthy VL, Quarta CC, Rapezzi C, Ruberg FL, Shah SJ, Slart RHJA, Verberne HJ, Bourque JM. ASNC/AHA/ASE/EANM/HFSA/ISA/SCMR/SNMMI expert consensus recommendations for multimodality imaging in cardiac amyloidosis: Part 2 of 2—Diagnostic criteria and appropriate utilization. J Nucl Cardiol. 2019;27(2):659–73.

45. Pozo E, Kanwar A, Deochand R, Castellano JM, Naib T, Pazos-López P, Osman K, Cham M, Narula J, Fuster V, Sanz J. Cardiac magnetic resonance evaluation of left ventricular remodelling distribution in cardiac amyloidosis. Heart. 2014;100(21):1688–95.

46. Carroll JD, Gaasch WH, McAdam KPWJ. Amyloid cardiomyopathy: Characterization by a distinctive voltage/mass relation. Am J Cardiol. 1982;49(1):9–13.

47. Maceira AM, Joshi J, Prasad SK, Moon JC, Perugini E, Harding I, Sheppard MN, Poole-Wilson PA, Hawkins PN, Pennell DJ. Cardiovascular magnetic resonance in cardiac amyloidosis. Circulation. 2005 Jan;111(2):186–93.

48. Vogelsberg H, Mahrholdt H, Deluigi CC, Yilmaz A, Kispert EM, Greulich S, Klingel K, Kandolf R, Sechtem U. Cardiovascular magnetic resonance in clinically suspected cardiac amyloidosis: noninvasive imaging compared to endomyocardial biopsy. J Am Coll Cardiol. 2008 Mar;51(10):1022–30.

49. Syed IS, Glockner JF, Feng D, Araoz PA, Martinez MW, Edwards WD, Gertz MA, Dispenzieri A, Oh JK, Bellavia D, Tajik AJ, Grogan M. Role of cardiac magnetic resonance imaging in the detection of cardiac amyloidosis. JACC Cardiovasc Imaging. 2010 Feb;3(2):155–64.

50. Karamitsos TD, Piechnik SK, Banypersad SM, Fontana M, Ntusi NB, Ferreira VM, Whelan CJ, Myerson SG, Robson MD, Hawkins PN, Neubauer S, Moon JC. Noncontrast T1 mapping for the diagnosis of cardiac amyloidosis. JACC Cardiovasc Imaging. 2013;6(4):488–97.

51. Martinez-Naharro A, Kotecha T, Norrington K, Boldrini M, Rezk T, Quarta C, et al. Native T1 and Extracellular Volume in Transthyretin Amyloidosis. JACC Cardiovasc Imaging. 2019;12(5):810–9.

52. Martinez-Naharro A, Abdel-Gadir A, Treibel TA, Zumbo G, Knight DS, Rosmini S, Lane T, Mahmood S, Sachchithanantham S, Whelan CJ, Lachmann HJ, Wechalekar AD, Kellman P, Gillmore JD, Moon JC, Hawkins PN, Fontana M. CMR-Verified Regression of Cardiac AL Amyloid After Chemotherapy. JACC Cardiovasc Imaging. 2018;11(1):152–4.

53. Gillmore JD, Maurer MS, Falk RH, Merlini G, Damy T, Dispenzieri A, Wechalekar AD, Berk JL, Quarta CC, Grogan M, Lachmann HJ, Bokhari S, Castano A, Dorbala S, Johnson GB, Glaudemans AWJM, Rezk T, Fontana M, Palladini G, Milani P, Guidalotti PL, Flatman K, Lane T, Vonberg FW, Whelan CJ, Moon JC, Ruberg FL, Miller EJ, Hutt DF, Hazenberg BP, Rapezzi C, Hawkins P. Nonbiopsy diagnosis of cardiac transthyretin amyloidosis. Circulation. 2016;133(24):2404–12.

54. Ortiz A, Germain DP, Desnick RJ, Politei J, Mauer M, Burlina A, Eng C, Hopkin RJ, Laney D, Linhart A, Waldek S, Wallace E, Weidemann F, Wilcox WR. Fabry disease revisited: Management and treatment recommendations for adult patients. Mol Genet Metab. 2018;123(4):416–27.

55. Baig S, Edward NC, Kotecha D, Liu B, Nordin S, Kozor R, Moon JC, Geberhiwot T, Steeds RP. Ventricular arrhythmia and sudden cardiac death in Fabry disease: a systematic review of risk factors in clinical practice. Europace. 2018;20(FI2):f153–61.

56. Omahony C, Coats C, Cardona M, Garcia A, Calcagnino M, Murphy E, Lachmann

R, Mehta A, Hughes D, Elliott PM. Incidence and predictors of anti-bradycardia pacing in patients with Anderson-Fabry disease. Europace. 2011;13(12):1781–8.

57. Cianciulli TF, Saccheri MC, Fernández SP, Fernández CC, Rozenfeld PA, Kisinovsky I. Apical left ventricular hypertrophy and mid-ventricular obstruction in Fabry disease. Echocardiography. 2015;32(5):860–3.

58. Calcagnino M, O'Mahony C, Coats C, Cardona M, Garcia A, Janagarajan K, Mehta A, Hughes D, Murphy E, Lachmann R, Elliott PM. Exercise-induced left ventricular outflow tract obstruction in symptomatic patients with Anderson-Fabry disease. J Am Coll Cardiol. 2011;58(1):88–9.

59. Tower-Rader A, Jaber WA. Multimodality imaging assessment of Fabry disease. Circ Cardiovasc Imaging. 2019;12(11):1–13.

60. Valent P, Klion AD, Roufosse F, Simon D, Metzgeroth G, Leiferman KM, Schwaab J, Butterfield JH, Sperr WR, Sotlar K, Vandenberghe P, Hoermann G, Haferlach T, Moriggl R, George TI, Akin C, Bochner BS, Gotlib J, Reiter A, Horny HP, Arock M, Simon HU, Gleich GJ. Proposed refined diagnostic criteria and classification of eosinophil disorders and related syndromes. Allergy Eur J Allergy Clin Immunol. 2023;78(1):47–59.

61. Salemi VMC, Rochitte CE, Shiozaki AA, Andrade JM, Parga JR, De Ávila LF, Benvenuti LA, Cestari IN, Picard MH, Kim RJ, Mady C. Late gadolinium enhancement magnetic resonance imaging in the diagnosis and prognosis of endomyocardial fibrosis patients. Circ Cardiovasc Imaging. 2011;4(3):304–11.

62. Gao M, Zhang W, Zhao W, Qin L, Pei F, Zheng Y. Loeffler endocarditis as a rare cause of heart failure with preserved ejection fraction. Med (United States). 2018;97(11):4–7.

63. Maron BJ. Clinical course and management of hypertrophic cardiomyopathy. N Engl J Med. 2018;379(7):655–68.

64. Maron BJ, Rowin EJ, Casey SA, Maron MS. How hypertrophic cardiomyopathy

became a contemporary treatable genetic disease with low mortality: Shaped by 50 years of clinical research and practice. JAMA Cardiol. 2016;1(1):98–105.

65. Zeppenfeld K, Tfelt-Hansen J, de Riva M, Winkel BG, Behr ER, Blom NA, Charron P, Corrado D, Dagres N, de Chillou C, Eckardt L, Friede T, Haugaa KH, Hocini M, Lambiase PD, Marijon E, Merino JL, Peichl P, Priori SG, Reichlin T, Schulz-Menger J, Sticherling C, Tzeis S, Verstrael A, Volterrani M, and ESC Scientific Document Group. 2022 ESC Guidelines for the management of patients with ventricular arrhythmias and the prevention of sudden cardiac death. Eur Heart J. 2022;1–130.

66. Kubo T, Kitaoka H. Imaging of Left Ventricular Hypertrophy: a Practical Utility for Differential Diagnosis and Assessment of Disease Severity. Curr Cardiol Rep. 2017;19(8).

67. Deva DP, Hanneman K, Li Q, Ng MY, Wasim S, Morel C, Iwanochko RM, Thavendiranathan P, Crean AM. Cardiovascular magnetic resonance demonstration of the spectrum of morphological phenotypes and patterns of myocardial scarring in Anderson-Fabry disease. J Cardiovasc Magn Reson. 2016;18(1):1–10.

68. Dungu JN, Valencia O, Pinney JH, Gibbs SDJ, Rowczenio D, Gilbertson JA, Lachmann HJ, Wechalekar A, Gillmore JD, Whelan CJ, Hawkins PN, Anderson LJ. CMR-based differentiation of AL and ATTR cardiac amyloidosis. JACC Cardiovasc Imaging. 2014;7(2):133–42.

69. Park CH, Chung H, Kim Y, Kim JY, Min PK, Lee KA, Yoon YW, Kim TH, Lee BK, Hong BK, Rim SJ, Kwon HM, Choi EY. Electrocardiography based prediction of hypertrophy pattern and fibrosis amount in hypertrophic cardiomyopathy: comparative study with cardiac magnetic resonance imaging. Int J Cardiovasc Imaging. 2018;34(10):1619–28.

70. Konno T, Nagata Y, Teramoto R, Fujino N, Nomura A, Tada H, Sakata K, Furusho H, Takamura M, Nakamura H, Kawashiri M, Yamagishi M, Hayashi K. Usefulness

of Electrocardiographic Voltage to Determine Myocardial Fibrosis in Hypertrophic Cardiomyopathy. Am J Cardiol. 2016;117(3):443–9.

71. Sakamoto N, Kawamura Y, Sato N, Nimura A, Matsuki M, Yamauchi A, Kanno T, Tanabe Y, Takeuchi T, Natori S, Saijo Y, Aburano T, Hasebe N. Late gadolinium enhancement on cardiac magnetic resonance represents the depolarizing and repolarizing electrically damaged foci causing malignant ventricular arrhythmia in hypertrophic cardiomyopathy. Hear Rhythm. 2015;12(6):1276–84.

72. Gersh BJ, Maron BJ, Bonow RO, Dearani JA, Fifer MA, Link MS, Naidu SS, Nishimura RA, Ommen SR, Rakowski H, Seidman CE, Towbin JA, Udelson JE, Yancy CW. 2011 ACCF/AHA guideline for the diagnosis and treatment of hypertrophic cardiomyopathy: A report of the American College of cardiology foundation/American heart association task force on practice guidelines. Circulation. 2011;124(24):783–831.

73. Doesch C, Tülümen E, Akin I, Rudic B, Kuschyk J, El-Battrawy I, Becher T, Budjan J, Smakic A, Schoenberg SO, Borggrefe M, Papavassiliu T. Incremental benefit of late gadolinium cardiac magnetic resonance imaging for risk stratification in patients with hypertrophic cardiomyopathy. Sci Rep. 2017;7(1):1–9.

74. Weng Z, Yao J, Chan RH, He J, Yang X, Zhou Y, He Y. Prognostic Value of LGE-CMR in HCM: A Meta-Analysis. JACC Cardiovasc Imaging. 2016;9(12):1392–402.

75. Hinojar R, Fernández-Golfín C, González-Gómez A, Rincón LM, Plaza-Martin M, Casas E, Garcia-Martin A, Fernandez-Mendez MA, Esteban A, Nacher JJJ, Zamorano JL. Prognostic implications of global myocardial mechanics in hypertrophic cardiomyopathy by cardiovascular magnetic resonance feature tracking. Relations to left ventricular hypertrophy and fibrosis. Int J Cardiol. 2017;249:467–72.

76. Smith BM, Dorfman AL, Yu S, Russell MW, Agarwal PP, Mahani MG, Lu JC. Relation of strain by feature tracking and clinical outcome in children, adolescents, and young adults with hypertrophic cardiomyopathy. Am J Cardiol. 2014;114(8):1275–80.

77. Alfakih K, Plein S, Thiele H, Jones T, Ridgway JP, Sivananthan MU. Normal human left and right ventricular dimensions for MRI as assessed by turbo gradient echo and steady-state free precession imaging sequences. J Magn Reson Imaging. 2003;17(3):323–9.

78. Csecs I, Czimbalmos C, Suhai FI, Mikle R, Mirzahosseini A, Dohy Z, Szűcs A, Kiss AR, Simor T, Tóth A, Merkely B, Vágó H. Left and right ventricular parameters corrected with threshold-based quantification method in a normal cohort analyzed by three independent observers with various training-degree. Int J Cardiovasc Imaging. 2018;34(7):1127–33.

79. Dohy Z, Szabo L, Pozsonyi Z, Csecs I, Toth A, Suhai FI, Czimbalmos C, Szucs A, Kiss AR, Becker D, Merkely B, Vago H. Potential clinical relevance of cardiac magnetic resonance to diagnose cardiac light chain amyloidosis. PLoS One. 2022;17(6 June):1–13.

80. Dohy Z, Csécs I, Czimbalmos C, Suhai FI, Tóth A, Szabó L, Pozsonyi Z, Simor T, Merkely B, Vágó H. Cardiac magnetic resonance „fingerprints" of cardiomyopathies with myocardial hypertrophy or increased left vent-ricular wall thickness. Cardiol Hungarica. 2018;48(6):390–6.

81. Dohy Z, Vereckei A, Horvath V, Czimbalmos C, Szabo L, Toth A, Suhai FI, Csecs I, Becker D, Merkely B, Vago H. How are ECG parameters related to cardiac magnetic resonance images? Electrocardiographic predictors of left ventricular hypertrophy and myocardial fibrosis in hypertrophic cardiomyopathy. Ann Noninvasive Electrocardiol. 2020;25(5):1–9.

82. Dohy Z, Szabo L, Toth A, Czimbalmos C, Horvath R, Horvath V, Suhai FI, Geller L, Merkely B, Vago H. Prognostic significance of cardiac magnetic resonance-

based markers in patients with hypertrophic cardiomyopathy. Int J Cardiovasc Imaging. 2021;37(6):2027–36.

83. Sievers B, Kirchberg S, Bakan A, Franken U, Trappe H-J. Impact of papillary muscles in ventricular volume and ejection fraction assessment by cardiovascular magnetic resonance. J Cardiovasc Magn Reson Off J Soc Cardiovasc Magn Reson. 2004;6(1):9–16.

84. Vogel-Claussen J, Finn JP, Gomes AS, Hundley GW, Jerosch-Herold M, Pearson G, Sinha S, Lima JAC, Bluemke DA. Left ventricular papillary muscle mass: Relationship to left ventricular mass and volumes by magnetic resonance imaging. J Comput Assist Tomogr. 2006;30(3):426–32.

85. Hudsmith LE, Petersen SE, Francis JM, Robson MD, Neubauer S. Normal human left and right ventricular and left atrial dimensions using steady state free precession magnetic resonance imaging. J Cardiovasc Magn Reson. 2005;7(5):775–82.

86. André F, Burger A, Loßnitzer D, Buss SJ, Abdel-Aty H, Gianntisis E, Steen H, Katus HA. Reference values for left and right ventricular trabeculation and non-compacted myocardium. Int J Cardiol. 2015;185:240–7.

87. Chuang ML, Gona P, Hautvast GLTF, Salton CJ, Blease SJ, Yeon SB, Breeuwer M, O'Donnell CJ, Manning WJ. Left Ventricular Trabeculae and Papillary Muscles: Correlation With Clinical and Cardiac Characteristics and Impact on Cardiovascular Magnetic Resonance Measures of Left Ventricular Anatomy and Function. JACC Cardiovasc Imaging. 2012;5(11):1115–23.

88. Papavassiliu T, Kühl HP, Schröder M, Süselbeck T, Bondarenko O, Böhm CK, Beek A, Hofman MMB, van Rossum AC. Effect of Endocardial Trabeculae on Left Ventricular Measurements and Measurement Reproducibility at Cardiovascular MR Imaging. Radiology. 2005;236:57–64.

89. Park EA, Lee W, Kim HK, Chung JW. Effect of papillary muscles and trabeculae on left ventricular measurement using cardiovascular magnetic resonance imaging

in patients with hypertrophic cardiomyopathy. Korean J Radiol. 2015;16(1):4–12.

90. Weinsaft JW, Cham MD, Janik M, Min JK, Henschke CI, Yankelevitz DF, Devereux RB. Left ventricular papillary muscles and trabeculae are significant determinants of cardiac MRI volumetric measurements: Effects on clinical standards in patients with advanced systolic dysfunction. Int J Cardiol. 2008;126(3):359–65.

91. Riffel JH, Schmucker K, Andre F, Ochs M, Hirschberg K, Schaub E, Fritz T, Mueller-Hennessen M, Giannitsis E, Katus HA, Friedrich MG. Cardiovascular magnetic resonance of cardiac morphology and function: impact of different strategies of contour drawing and indexing. Clin Res Cardiol. 2019;108(4):411–29.

92. Levy D, Garrison RJ, Savage DD, Kannel WB, Castelli WP. Prognostic implications of echocardiographically determined left ventricular mass in the Framingham Heart Study. New English J Med. 1990;323(16):1120–3.

93. Bluemke DA, Kronmal RA, Lima JAC, Liu K, Olson J, Burke GL, Folsom AR. The relationship of left ventricular mass and geometry to incident cardiovascular events: The MESA Study. 2009;52(25):2148–55.

94. De Groote P, Millaire A, Foucher-Hossein C, Nugue O, Marchandise X, Ducloux G, Lablanche JM. Right ventricular ejection fraction is an independent predictor of survival in patients with moderate heart failure. J Am Coll Cardiol. 1998;32(4):948–54.

95. Di Salvo TG, Mathier M, Semigran MJ, Dec GW. Preserved right ventricular ejection fraction predicts exercise capacity and survival in advanced heart failure. J Am Coll Cardiol. 1995;25(5):1143–53.

96. Driessen MMP, Baggen VJM, Freling HG, Pieper PG, Van Dijk AP, Doevendans PA, Snijder RJ, Post MC, Meijboom FJ, Sieswerda GT, Leiner T, Willems TP. Pressure overloaded right ventricles: A multicenter study on the importance of trabeculae in RV function measured by CMR. Int J Cardiovasc Imaging.

2014;30(3):599–608.

97. Polak JF, Holman BL, Wynne J, Colucci WS. Right ventricular ejection fraction: An indicator of increased mortality in patients with congestive heart failure associated with coronary artery disease. J Am Coll Cardiol. 1983;2(2):217–24.

98. Kawut SM, Horn EM, Berekashvili KK, Garofano RP, Goldsmith RL, Widlitz AC, Rosenzweig EB, Kerstein D, Barst RJ. New predictors of outcome in idiopathic pulmonary arterial hypertension. Am J Cardiol. 2005;95(2):199–203.

99. Goldhaber SZ, Visani L, De Rosa M. Acute pulmonary embolism: Clinical outcomes in the International Cooperative Pulmonary Embolism Registry (ICOPER). Lancet. 1999;353(9162):1386–9.

100. Pan JA, Kerwin MJ, Salerno M. Native T1 Mapping, Extracellular Volume Mapping, and Late Gadolinium Enhancement in Cardiac Amyloidosis: A Meta-Analysis. JACC Cardiovasc Imaging. 2020;13(6):1299–310.

101. Zhao L, Tian Z, Fang Q. Diagnostic accuracy of cardiovascular magnetic resonance for patients with suspected cardiac amyloidosis: A systematic review and meta-analysis. BMC Cardiovasc Disord. 2016;16(1):1–10.

102. Ruberg FL, Appelbaum E, Davidoff R, Ozonoff A, Kissinger K V, Harrigan C, Skinner M, Manning WJ. Diagnostic and prognostic utility of cardiovascular magnetic resonance imaging in light-chain cardiac amyloidosis. Am J Cardiol. 2009 Feb;103(4):544–9.

103. Austin BA, Tang WHW, Rodriguez ER, Tan C, Flamm SD, Taylor DO, Starling RC, Desai MY. Delayed hyper-enhancement magnetic resonance imaging provides incremental diagnostic and prognostic utility in suspected cardiac amyloidosis. JACC Cardiovasc Imaging. 2009 Dec;2(12):1369–77.

104. Williams LK, Forero JF, Popovic ZB, Phelan D, Delgado D, Rakowski H, Wintersperger BJ, Thavendiranathan P. Patterns of CMR measured longitudinal strain and its association with late gadolinium enhancement in patients with cardiac

amyloidosis and its mimics. J Cardiovasc Magn Reson. 2017;19(1):1–10.

105. Pandey T, Alapati S, Wadhwa V, Edupuganti MM, Gurram P, Lensing S, Jambhekar K. Evaluation of Myocardial Strain in Patients With Amyloidosis Using Cardiac Magnetic Resonance Feature Tracking. Curr Probl Diagn Radiol. 2017;46(4):288–94.

106. Bhatti S, Vallurupalli S, Ambach S, Magier A, Watts E, Truong V, Hakeem A, Mazur W. Myocardial strain pattern in patients with cardiac amyloidosis secondary to multiple myeloma: a cardiac MRI feature tracking study. Int J Cardiovasc Imaging. 2018;34(1):27–33.

107. Mathur S, Dreisbach JG, Karur GR, Iwanochko RM, Morel CF, Wasim S, Nguyen ET, Wintersperger BJ, Hanneman K. Loss of base-to-apex circumferential strain gradient assessed by cardiovascular magnetic resonance in Fabry disease: Relationship to T1 mapping, late gadolinium enhancement and hypertrophy. J Cardiovasc Magn Reson. 2019;21(1):1–10.

108. Wilson HC, Ambach S, Madueme PC, Khoury PR, Hopkin RJ, Jefferies JL. Comparison of Native T1, Strain, and Traditional Measures of Cardiovascular Structure and Function by Cardiac Magnetic Resonance Imaging in Patients With Anderson-Fabry Disease. Am J Cardiol. 2018;122(6):1074–8.

109. Augusto JB, Johner N, Shah D, Nordin S, Knott KD, Rosmini S, Lau C, Alfarih M, Hughes R, Seraphim A, Vijapurapu R, Bhuva A, Lin L, Ojrzynska N, Geberhiwot T, Captur G, Ramaswami U, Steeds RP, Kozor R, Hughes D, Moon JC, Namdar M. The myocardial phenotype of Fabry disease pre-hypertrophy and pre-detectable storage. Eur Hear J - Cardiovasc Imaging. 2020;1–10.

110. Vijapurapu R, Nordin S, Baig S, Liu B, Rosmini S, Augusto J, Tchan M, Hughes DA, Geberhiwot T, Moon JC, Steeds RP, Kozor R. Global longitudinal strain, myocardial storage and hypertrophy in Fabry disease. Heart. 2019;105(6):470–6.

111. Haland TF, Almaas VM, Hasselberg NE, Saberniak J, Leren IS, Hopp E, Edvardsen T, Haugaa KH. Strain echocardiography is related to fibrosis and

ventricular arrhythmias in hypertrophic cardiomyopathy. Eur Heart J Cardiovasc Imaging. 2016;17(6):613–21.

112. Candan O, Gecmen C, Bayam E, Guner A, Celik M, Doğan C. Mechanical dispersion and global longitudinal strain by speckle tracking echocardiography: Predictors of appropriate implantable cardioverter defibrillator therapy in hypertrophic cardiomyopathy. Echocardiography. 2017 Jun;34(6):835–42.

113. Popa-Fotea N-M, Micheu MM, Onciul S, Zamfir D, Dorobanţu M. Combined right and left ventricular mechanical dispersion enhance the arrhythmic risk stratification in hypertrophic cardiomyopathy. J Cardiol. 2020 Oct;76(4):364–70.

114. Cianciulli TF, Saccheri MC, Rísolo MA, Lax JA, Méndez RJ, Morita LA, Beck MA, Kazelián LR. Mechanical dispersion in Fabry disease assessed with speckle tracking echocardiography. Echocardiography. 2020;37(2):293–301.

115. Gastl M, Behm P, Jacoby C, Kelm M, Bönner F. Multiparametric cardiac magnetic resonance imaging (CMR) for the diagnosis of Loeffler's endocarditis: A case report. BMC Cardiovasc Disord. 2017;17(1):1–4.

116. Yamamoto T, Tanaka H, Kurimoto C, Imanishi T, Hayashi N, Saegusa J, Morinobu A, Hirata K, Kawano S. Very early stage left ventricular endocardial dysfunction of patients with hypereosinophilic syndrome. Int J Cardiovasc Imaging. 2016;32(9):1357–61.

117. Feisst A, Kuetting DLR, Dabir D, Luetkens J, Homsi R, Schild HH, Thomas D. Influence of observer experience on cardiac magnetic resonance strain measurements using feature tracking and conventional tagging. Int J Cardiol Hear Vasc. 2018 Mar;18:46–51.

118. Mangion K, Burke NMM, McComb C, Carrick D, Woodward R, Berry C. Feature-tracking myocardial strain in healthy adults- a magnetic resonance study at 3.0 tesla. Sci Rep. 2019;9(1):1–9.

119. Almutairi HM, Boubertakh R, Miquel ME, Petersen SE. Myocardial deformation

assessment using cardiovascular magnetic resonance-feature tracking technique. Br J Radiol. 2017;90(1080).

120. Chen X, Zhao T, Lu M, Yin G, Xiangli W, Jiang S, Prasad S, Zhao S. The relationship between electrocardiographic changes and CMR features in asymptomatic or mildly symptomatic patients with hypertrophic cardiomyopathy. Int J Cardiovasc Imaging. 2014;30(SUPPL. 1):55–63.

121. Grossman A, Prokupetz A, Koren-Morag N, Grossman E, Shamiss A. Comparison of usefulness of Sokolow and Cornell criteria for left ventricular hypertrophy in subjects aged <20 years versus >30 years. Am J Cardiol. 2012;110(3):440–4.

122. Inoue YY, Ambale-Venkatesh B, Mewton N, Volpe GJ, Ohyama Y, Sharma RK, Wu CO, Liu CY, Bluemke DA, Soliman EZ, Lima JA, Ashikaga H. Electrocardiographic impact of myocardial diffuse fibrosis and scar: MESA (Multi-Ethnic study of atherosclerosis. Radiology. 2017;282(3):690–8.

123. Femenía F, Arce M, Van Grieken J, Trucco E, Mont L, Abello M, Merino JL, Rivero-Ayerza M, Gorenek B, Rodriguez C, Hopman WM, Baranchuk A. Fragmented QRS as a predictor of arrhythmic events in patients with hypertrophic obstructive cardiomyopathy. J Interv Card Electrophysiol. 2013;38(3):159–65.

124. Özyılmaz S, Akgül Ö, Uyarel H, Pusuroğlu H, Karayakalı M, Gül M, Cetin M, Satilmisoglu H, Yildirim A, Bakir I. Assessment of the association between the presence of fragmented qrs and the predicted risk score of sudden cardiac death at 5 years in patients with hypertrophic cardiomyopathy. Anatol J Cardiol. 2017;18(1):54–61.

125. Nomura N, Tani T, Konda T, Kim K, Kitai T, Nomoto N, Suganuma N, Nakamura H, Sumida T, Fujii Y, Kawai J, Kaji S, Furukawa Y. Significance of isolated papillary muscle hypertrophy: A comparison of left ventricular hypertrophy diagnosed using electrocardiography vs echocardiography. Echocardiography. 2018;35(3):292–300.

126. Rodrigues JCL, Amadu AM, Dastidar AG, McIntyre B, Szantho G V., Lyen S,

Godsave C, Ratcliffe LEK, Burchell AE, Hart EC, Hamilton MCK, Nightingale AK, Paton JFR, Manghat NE, Bucciarelli-Ducci C. ECG strain pattern in hypertension is associated with myocardial cellular expansion and diffuse interstitial fibrosis: A multi-parametric cardiac magnetic resonance study. Eur Heart J Cardiovasc Imaging. 2017;18(4):441–50.

127. Shah ASV, Chin CWL, Vassiliou V, Cowell SJ, Doris M, Kwok TC, Semple S, Zamvar V, White AC, McKillop G, Boon NA, Prasad SK, Mills NL, Newby DE, Dweck MR. Left ventricular hypertrophy with strain and aortic stenosis. Circulation. 2014;130(18):1607–16.

128. Terho HK, Tikkanen JT, Junttila JM, Anttonen O, Kenttä T V., Aro AL, Kerola T, Rissanen HA, Reunanen A, Huikuri HV. Prevalence and prognostic significance of fragmented QRS complex in middle-aged subjects with and without clinical or electrocardiographic evidence of cardiac disease. Am J Cardiol. 2014;114(1):141–7.

129. He D, Ye M, Zhang L, Jiang B. Prognostic significance of late gadolinium enhancement on cardiac magnetic resonance in patients with hypertrophic cardiomyopathy. Hear Lung. 2018;47(2):122–6.

130. Green JJ, Berger JS, Kramer CM, Salerno M. Prognostic value of late gadolinium enhancement in clinical outcomes for hypertrophic cardiomyopathy. JACC Cardiovasc Imaging. 2012;5(4):370–7.

131. O'Mahony C, Jichi F, Pavlou M, Monserrat L, Anastasakis A, Rapezzi C, Biagini E, Gimeno JR, Limongelli G, McKenna WJ, Omar RZ, Elliott PM. A novel clinical risk prediction model for sudden cardiac death in hypertrophic cardiomyopathy (HCM Risk-SCD). Eur Heart J. 2014;35(30):2010–20.

132. Spirito P, Bellone P, Harris KM, Bernabò P, Bruzzi P, Maron BJ. Magnitude of Left Ventricular Hypertrophy and Risk of Sudden Death in Hypertrophic Cardiomyopathy. N Engl J Med. 2000;342(24):1778–85.

133. Elliott PM, Gimeno Blanes JR, Mahon NG, Poloniecki JD, McKenna WJ. Relation

between severity of left-ventricular hypertrophy and prognosis in patients with hypertrophic cardiomyopathy. Lancet. 2001;357(9254):420–4.

134. Olivotto I, Gistri R, Petrone P, Pedemonte E, Vargiu D, Cecchi F. Maximum left ventricular thickness and risk of sudden death in patients with hypertrophic cardiomyopathy. J Am Coll Cardiol. 2003;41(2):315–21.

135. Śpiewak M, Chojnowska L, Małek ŁA, Miłosz B, Petryka J, Zabicka M, Klopotowski M, Dabrowski M, Misko J, Ruzyllo W. Comparison between maximal left ventricular wall thickness and left ventricular mass in patients with hypertrophic cardiomyopathy. Kardiol Pol. 2010;68(7):763–8.

136. Olivotto I, Maron MS, Autore C, Lesser JR, Rega L, Casolo G, De Santis M, Quarta G, Nistri S, Cecchi F, Salton CJ, Udelson JE, Manning WJ, Maron BJ. Assessment and Significance of Left Ventricular Mass by Cardiovascular Magnetic Resonance in Hypertrophic Cardiomyopathy. J Am Coll Cardiol. 2008;52(7):559–66.

137. Armstrong AC, Gidding S, Gjesdal O, Wu C, Bluemke DA, Lima JAC. LV mass assessed by echocardiography and CMR, cardiovascular outcomes, and medical practice. JACC Cardiovasc Imaging. 2012;5(8):837–48.

138. Saito M, Okayama H, Yoshii T, Higashi H, Morioka H, Hiasa G, Sumimoto T, Inaba S, Nishimura K, Inoue K, Ogimoto A, Shigematsu Y, Hamada M, Higaki J. Clinical significance of global two-dimensional strain as a surrogate parameter of myocardial fibrosis and cardiac events in patients with hypertrophic cardiomyopathy. Eur Heart J Cardiovasc Imaging. 2012;13(7):617–23.

139. Reant P, Mirabel M, Lloyd G, Peyrou J, Lopez Ayala JM, Dickie S, Bulluck H, Captur G, Rosmini S, Guttmann O, Demetrescu C, Pantazis A, Tome-Esteban M, Moon JC, Lafitte S, McKenna WJ. Global longitudinal strain is associated with heart failure outcomes in hypertrophic cardiomyopathy. Heart. 2016;102(10):741–7.

140. Muser D, Tioni C, Shah R, Selvanayagam JB, Nucifora G. Prevalence, Correlates,

and Prognostic Relevance of Myocardial Mechanical Dispersion as Assessed by Feature-Tracking Cardiac Magnetic Resonance After a First ST-Segment Elevation Myocardial Infarction. Am J Cardiol. 2017;120(4):527–33.

## 10. Bibliography of the candidate's publications

### 10.1. Publications related to the PhD thesis

[1] ***Dohy Z***, Szabo L, Pozsonyi Z, Csecs I, Toth A, Suhai FI, Czimbalmos C, Szucs A, Kiss AR, Becker D, Merkely B, Vago H. Potential clinical relevance of cardiac magnetic resonance to diagnose cardiac light chain amyloidosis. PLOS ONE. 2022;17(6 June):1–13. **IF: 3.752**

[2] ***Dohy Z***, Szabo L, Toth A, Czimbalmos C, Horvath R, Horvath V, Suhai FI, Geller L, Merkely B, Vago H. Prognostic significance of cardiac magnetic resonance-based markers in patients with hypertrophic cardiomyopathy. INTERNATIONAL JOURNAL OF CARDIOVASCULAR IMAGING. 2021;37(6):2027–36. **IF: 2.316**

[3] ***Dohy Z***, Vereckei A, Horvath V, Czimbalmos C, Szabo L, Toth A, Suhai FI, Csecs I, Becker D, Merkely B, Vago H. How are ECG parameters related to cardiac magnetic resonance images? Electrocardiographic predictors of left ventricular hypertrophy and myocardial fibrosis in hypertrophic cardiomyopathy. ANNALS OF NONINVASIVE ELECTROCARDIOLOGY. 2020;25(5):1–9. **IF: 1.468**

[4] Csecs I, Czimbalmos C, Suhai FI, Mikle R, Mirzahosseini A, ***Dohy Z***, Szűcs A, Kiss AR, Simor T, Tóth A, Merkely B, Vágó H. Left and right ventricular parameters corrected with threshold-based quantification method in a normal cohort analyzed by three independent observers with various training-degree. INTERNATIONAL JOURNAL OF CARDIOVASCULAR IMAGING. 2018;34(7):1127–33. **IF: 1.860**

[5] ***Dohy Z***, Csécs I, Czimbalmos C, Suhai FI, Tóth A, Szabó L, Pozsonyi Z, Simor T, Merkely B, Vágó H. Balkamra-hipertrófiával, illetve megnövekedett falvastagsággal járó cardiomyopathiák szív mágneses rezonanciás jellegzetességei [Cardiac magnetic resonance „fingerprints" of cardiomyopathies with myocardial hypertrophy or increased left vent-ricular wall thickness]. CARDIOLOGIA HUNGARICA. 2018;48(6):390–6.

### 10.2. Publications not related to the PhD Thesis

[1] Grebur K, Gregor Z, Kiss AR, Horváth M, Mester B, Czimbalmos C, Tóth A, Szabó LE, ***Dohy Z***, Vágó H, Merkely B, Szűcs A. Different methods, different results? Threshold-based versus conventional contouring techniques in clinical practice. INTERNATIONAL JOURNAL OF CARDIOLOGY, 2023;381 128-34. **IF: 4.039**

[2] Szabo L, Brunetti G, Cipriani A, Juhasz V, Graziano F, Hirschberg K, ***Dohy Z***, Balla D, Drobni Z, Perazzolo Marra M, Corrado D, Merkely B, Zorzi A, Vago H. Certainties and Uncertainties of Cardiac Magnetic Resonance Imaging in Athletes. JOURNAL OF CARDIOVASCULAR DEVELOPMENT AND DISEASE, 2022 Oct 20;9(10):361. **IF: 4.415**

[3] Skoda R, Juhász V, ***Dohy Z***, Pintér A, Bokor L, Bárczi G, Vágó H, Merkely B, Becker D. The effect of COVID-19 pandemic on myocardial infarction care and on its prognosis - Experience at a high volume Hungarian cardiovascular center. PHYSIOLOGY INTERNATIONAL, 2022 Sep 5;109(3):419-26. **IF: 1.697**

[4] Vago H, Szabo L, Szabo Z, Ulakcsai Z, Szogi E, Budai G, Toth A, Juhasz V, ***Dohy Z***, Hoffer K, Becker D, Kiss RG, Nagy GG, Nagy G, Merkely B. Immunological response and temporal associations in myocarditis after COVID-19 vaccination using cardiac magnetic resonance imaging: an amplified T-cell response at the heart of it? FRONTIERS IN CARDIOVASCULAR MEDICINE, 2022 Sep 15;9:961031. **IF: 5.848**

[5] Ocsovszky Z, Otohal J, Berényi B, Juhász V, Skoda R, Bokor L, ***Dohy Z***, Szabó L, Nagy G, Becker D, Merkely B, Vágó H. The associations of long-COVID symptoms, clinical characteristics and affective psychological constructs in a non-hospitalized cohort. PHYSIOLOGY INTERNATIONAL, 2022;109(2) 230-45. **IF: 1.697**

[6] Kiss AR, Gregor Z, Popovics A, Grebur K, Szabó LE, ***Dohy Z***, Kovács A, Lakatos BK, Merkely B, Vágó H, Szũcs A: Impact of Right Ventricular Trabeculation on Right Ventricular Function in Patients With Left Ventricular Non-compaction Phenotype. FRONTIERS IN CARDIOVASCULAR MEDICINE, 2022 Apr 12;9:843952. **IF: 5.848**

[7] Budai A, Suhai FI, Csorba K, ***Dohy Z***, Szabo L, Merkely B, Vago H: Automated Classification of Left Ventricular Hypertrophy on Cardiac MRI. APPLIED SCIENCES, 2022 ; 12(9):4151. **IF: 2.838**

[8] ***Dohy Z***, Fekete B, Csoka K, Nagy B, Fintha A, Szabo L, Juhasz V, Czibor S, Balla D, Tomcsanyi J, Karlocai K, Matolcsy A, Merkely B, Bodor C, Vago H: Az aritmogén cardiomyopathia szokatlan megjelenési formái. Amikor a genetika segít [Uncommon presentations of arrhythmogenic cardiomyopathy – when genetic testing helps]. CARDIOLOGIA HUNGARICA, 2022; 52: 33-7.

[9] Nagy B, Csonka K, Fekete B, Dohy Z, Szabo L, Fintha A, Matolcsy A, Merkely B, Vago H, Bodor C: Genetikai vizsgálatok örökletes kardiovaszkuláris betegségekben [Genetic testing in hereditary cardiovascular diseases]. CARDIOLOGIA HUNGARICA, 2022; 52: 23-32.

[10] Szabó L, Juhász V, ***Dohy Z***, Fogarasi C, Kovács A, Lakatos BK, Kiss O, Sydó N, Csulak E, Suhai FI, Hirschberg K, Becker D, Merkely B, Vágó H: Is cardiac involvement prevalent in highly trained athletes after SARS-CoV-2 infection? A cardiac magnetic resonance study using sex-matched and age-matched controls. BRITISH JOURNAL OF SPORTS MEDICINE, 2021 May;56(10):553-560. **IF: 18.479**

[11] Kiss O, Babity M, Kovacs A, Skopal J, Vago H, Lakatos BK, Bognar C, Rakoczi R, Zamodics M, Frivaldszky L, Menyhart-Hetenyi A, ***Dohy Z***, Czimbalmos C, Szabo L, Merkely B. Significance of extended sports cardiology screening of elite handball referees. PLOS ONE, 2021 Apr 9;16(4):e0249923. **IF: 3.752**

[12] Vago H, Szabo L, ***Dohy Z***, Merkely B. Cardiac magnetic resonance findings in patients recovered from COVID-19: initial experiences in elite athletes. JACC CARDIOVASCULAR IMAGING 2021 Jun;14(6):1279-81. *Reserarch Letter* **IF: 16.051**

[13] Brenner GB, Giricz Z, Garamvölgyi R, Makkos A, Onódi Z, Sayour NV, Gergely TG, Baranyai T, Petneházy Ö, Kőrösi D, Szabó GP, Vago H, ***Dohy Z***, Czimbalmos C, Merkely B, Boldin-Adamsky S, Feinstein E, Horváth IG, Ferdinandy P. Post-Myocardial Infarction Heart Failure in Closed-chest Coronary Occlusion/Reperfusion Model in

Göttingen Minipigs and Landrace Pigs. JOURNAL OF VISUALIZED EXPERIMENTS, 2021 Apr 17;(170). **IF: 1.424**

[14] Kiss AR, Gregor Z, Furák Á, Szabó LE, ***Dohy*** Z, Merkely B, Vágó H, Szűcs A. Age- and Sex-Specific Characteristics of Right Ventricular Compacted and Non-compacted Myocardium by Cardiac Magnetic Resonance. FRONTIERS IN CARDIOVASCULAR MEDICINE, 2021 Dec 7;8:781393. **IF: 5.848**

[15] Kiss AR, Gregor Z, Furak A, Tóth A, Horváth M, Szabo L, Czimbalmos C, ***Dohy Z***, Merkely B, Vago H, Szucs A. Left ventricular characteristics of noncompaction phenotype patients with good ejection fraction measured with cardiac magnetic resonance. ANATOLIAN JOURNAL OF CARDIOLOGY, 2021 Aug;25(8):565-71. **IF: 1.475**

[16] Csulak E, Petrov Á, Kováts T, Tokodi M, Lakatos B, Kovács A, Staub L, Suhai FI, Szabó EL, ***Dohy Z***, Vágó H, Becker D, Müller V, Sydó N, Merkely B. The Impact of COVID-19 on the Preparation for the Tokyo Olympics: A Comprehensive Performance Assessment of Top Swimmers. INTERNATIONAL JOURNAL OF ENVIRONMENTAL RESEARCH AND PUBLIC HEALTH, 2021 Sep 16;18(18):9770. **IF: 4.614**

[17] Gregor Z, Kiss AR, Szabó LE, Tóth A, Grebur K, Horváth M, ***Dohy Z***, Merkely B, Vágó H, Szűcs A. Sex- and age-specific normal values of left ventricular functional and myocardial mass parameters using threshold-based trabeculae quantification. PLOS ONE, 2021 Oct 12;16(10):e0258362. **IF: 3.752**

[18] Szűcs A, Kiss AR, Gregor Z, Horváth M, Tóth A, Dohy Z, Szabó LE, Suhai FI, Merkely B, Vágó H. Changes in strain parameters at different deterioration levels of left ventricular function: A cardiac magnetic resonance feature-tracking study of patients with left ventricular noncompaction. INTERNATIONAL JOURNAL OF CARDIOLOGY, 2021 May 15;331:124-30. **IF: 4.039**

[19] Szabó L, Juhász V, ***Dohy Z***, Hirschberg K, Czimbalmos C, Tóth A, Suhai FI, Merkely B, Vágó H. A szív mágneses rezonanciás vizsgálatának szerepe lezajlott

COVID-19-fertőzést követően [The role of cardiac magentic resonanca imaging after COVID-19 infection]. CARDIOLOGIA HUNGARICA, 2021; 51: 18-22.

[20] Pozsonyi Z, Pesko G, Czibor S, ***Dohy Z***, Vago H. A képalkotó vizsgálatok szerepe szívamyloidosis kivizsgálásában [Role of imaging modalities in diagnosing cardiac amyloidosis]. CARDIOLOGIA HUNGARICA, 2021; 51: 23-32.

[21] Vago H, Czimbalmos C, Papp R, Szabo L, Toth A, ***Dohy Z***, Csecs I, Suhai F, Kosztin A, Molnar L, Geller L, Merkely B. Biventricular pacing during cardiac magnetic resonance imaging. EUROPACE, 2020 Jan 1;22(1):117-24. **IF: 5.214**

[22] Vágó H, Szabó L, ***Dohy Z***, Czimbalmos C, Tóth A, Suhai FI, Bárczi G, Gyarmathy VA, Becker D, Merkely B. Early cardiac magnetic resonance imaging in troponin-positive acute chest pain and non-obstructed coronary arteries. BMJ HEART, 2020 Jul;106(13):992-1000. **IF: 5.994**

[23] Lakatos BK, Molnár AÁ, Kiss O, Sydó N, Tokodi M, Solymossi B, Fábián A, ***Dohy Z***, Vágó H, Babity M, Bognár C, Kovács A, Merkely B. Relationship between Cardiac Remodeling and Exercise Capacity in Elite Athletes: Incremental Value of Left Atrial Morphology and Function Assessed by Three-Dimensional Echocardiography. JOURNAL OF THE AMERICAN SOCIETY OF ECHOCARDIOGRAPHY, 2020 Jan;33(1):101-9.e1. **IF: 5.251**

[24] Csecs I, Czimbalmos C, Toth A, ***Dohy Z***, Suhai IF, Szabo L, Kovacs A, Lakatos B, Sydo N, Kheirkhahan M, Peritz D, Kiss O, Merkely B, Vago H. The impact of sex, age and training on biventricular cardiac adaptation in healthy adult and adolescent athletes: Cardiac magnetic resonance imaging study. EUROPEAN JOURNAL OF PREVENTIVE CARDIOLOGY, 2020 Mar;27(5):540-9. **IF: 7.804**

[25] Hirschberg K, ***Dohy Z***, Tóth A, Szabó L, Czimbalmos C, Finster M, Suhai F, Merkely B, Vágó H. A mappingtechnikák által nyújtott lehetőségek a szív-MR-vizsgálatok során: indikációk, diagnosztikus érték, limitációk és centrumunk kezdeti tapasztalatai [The potential of mapping techniques in cardiac magnetic resonance

imaging: Indications, diagnostic value, limitations and first experience in our center] CARDIOLOGIA HUNGARICA, 2020; 50: 47-55.

[26] Czimbalmos C, Csecs I, Toth A, Kiss O, Suhai FI, Sydo N, ***Dohy Z***, Apor A, Merkely B, Vago H. The demanding grey zone: Sport indices by cardiac magnetic resonance imaging differentiate hypertrophic cardiomyopathy from athlete's heart. PLOS ONE, 2019 Feb 14;14(2):e0211624. **IF: 2.740**

[27] Szűcs A, Kiss AR, Suhai FI, Tóth A, Gregor Z, Horváth M, Czimbalmos C, Csécs I, ***Dohy Z***, Szabó LE, Merkely B, Vágó H. The effect of contrast agents on left ventricular parameters calculated by a threshold-based software module: does it truly matter? INTERNATIONAL JOURNAL OF CARDIOVASCULAR IMAGING, 2019 Sep;35(9):1683-9. **IF: 1.969**

[28] Czimbalmos C, Csecs I, ***Dohy Z***, Toth A, Suhai FI, Müssigbrodt A, Kiss O, Geller L, Merkely B, Vago H. Cardiac magnetic resonance based deformation imaging: role of feature tracking in athletes with suspected arrhythmogenic right ventricular cardiomyopathy. INTERNATIONAL JOURNAL OF CARDIOVASCULAR IMAGING, 2019 Mar;35(3):529-38. **IF: 1.969**

[29] Czimbalmos C, Csécs I, Tóth A, Suhai FI, ***Dohy Z***, Szabó LE, Bárczi G, Zima E, Becker D, Merkely B, Vágó H. ST-elevációs miokardiális infarktus szív mágneses rezonanciás jellegzetességei az akut szakban és utánkövetés során. A mikrovaszkuláris obstrukció prognosztikus szerepe [Cardiac magnetic resonance characteristics of ST-segment elevation myocardial infarction in the acute period and during long-term follow up – prognostic role of microvascular obstruction]. CARDIOLOGIA HUNGARICA, 2018; 48: 308-12.

[30] Szabó L, Pozsonyi Z, Peskó G, ***Dohy Z***, Czimbalmos C, Heltai K, Becker D, Merkely B, Vágó H. Abortált hirtelen szívhalál egy 39 éves biztonsági őrnél [Aborted sudden cardiac death in a 39-year-old security guard]. CARDIOLOGIA HUNGARICA, 2018; 48: 197-400.

DOI:10.14753/SE.2024.2908

## 11. Acknowledgements

I would like to express my gratitude to all, who made this PhD thesis possible.

First and foremost, I would like to thank my supervisor Hajnalka Vágó for her guidance, positive energy, and continued support during my student research and PhD fellowship years. She was the one who made me love the world of cardiac MR and the beauty and difficulty of research.

I would like to express my appreciation to Prof. Béla Merkely for giving me the opportunity to carry out my research projects and providing the background required for my research.

I am grateful to Liliána Szabó, Csilla Czimbalmos, Ibolya Csécs, Vencel Juhász, Zsófia Drobni, Anna Kiss and Zsófia Gregor, who provided the much need advice and moral support during my PhD years.

I would like to also thank all the student researchers, especially Rebeka Horváth, Fanni Bátyi, and Viktor Horváth for their hard work and contribution.

I would like to thank to András Vereckei and Zoltán Pozsonyi for joining and supporting my research work.

I am thankful for the exceptional CMR team at Semmelweis University Heart and Vascular Center, most importantly Attila Tóth, Ferenc Imre Suhai, Éva Lehotai, and Piroska Bajorné.

Finally, I would like to thank my family (Máté Ficzere, Gábor Dohy, Rita Hudáky, Anna Dohy, Balázs Dohy), and my friends for their continuing love, patience, and support.